

**Some properties of the ferromagnetic XXZ spin chain  
and their applications to quantum computation**

By

JAIDEEP S. MULHERKAR

B.E. Electronics and telecommunications (University of Mumbai, India) 1993

M.S. Mathematics (California State Hayward, California) 2005

DISSERTATION

Submitted in partial satisfaction of the requirements for the degree of

DOCTOR OF PHILOSOPHY

in

Mathematics

in the

OFFICE OF GRADUATE STUDIES

of the

UNIVERSITY OF CALIFORNIA

DAVIS

Approved:

---

Bruno Nachtergaele (Chair)

---

Greg Kuperberg

---

Alexander Soshnikov

Committee in Charge

2009

To Poonam for her love and kind support

# Contents

Abstract	v
Acknowledgments	vi
Chapter 1. Introduction	1
1.1. Overview and motivation	1
1.2. Summary of results	2
Chapter 2. Preliminaries	5
2.1. Spin	5
2.2. Quantum Mechanics	6
2.3. XXZ Model	10
2.4. Quantum gates	15
2.5. Optimal Control Theory	17
2.6. Density Matrix Renormalization Group Algorithm	23
Chapter 3. Isolated Eigenvalues	31
3.1. Introduction	31
3.2. Set-up	33
3.3. Main theorem	36
3.4. Proof of Theorems 3.3.1 and 3.3.2 (Excitations of the Ising Model)	39
3.5. Proof of the main theorem	44
Chapter 4. Implementing gates	51
4.1. Introduction	51
4.2. Quantum gates using quantum control	54
4.3. DMRG simulations for quantum gates	59
4.4. Results	61

Appendix A. Code	66
Bibliography	73

Some properties of the ferromagnetic XXZ spin chain  
and their applications to quantum computation

**Abstract**

One of the key requirements of quantum computation is the ability to encode qubits and construct unitary gates that are protected from the effects of environmental noise. The ferromagnetic XXZ chain is one of the best studied quantum spin models. In this thesis we extend the study of the low lying spectrum of the one dimensional ferromagnetic XXZ chain with special boundary conditions by proving the existence of isolated interface states called ‘kinks’. We then capitalize on the isolated nature of these kink states to use them to encode a qubit and construct an implementation scheme for quantum gates.

In chapter 3 we investigate the low-lying excited states of the spin  $J$  ferromagnetic XXZ chain with Ising anisotropy  $\Delta$  and kink boundary conditions. Since the third component of the total magnetization,  $M$ , is conserved, it is meaningful to study the spectrum for each fixed value of  $M$ . In this chapter we prove that for  $J \geq 3/2$  and sufficiently large  $\Delta$ , the lowest excited eigenvalues of the XXZ chain determined by a fixed value of  $M$  are separated by a gap from the rest of the spectrum, uniformly in the length of the chain.

The existence of isolated eigenvalues in the low energy spectrum is very good from a quantum computing point of view since they provide natural protection from the noise effects. In chapter 4 we demonstrate an implementation scheme for constructing quantum gates using unitary evolutions of the one-dimensional spin- $J$  ferromagnetic XXZ chain. We present numerical results based on simulations of the chain using the time-dependent DMRG method and techniques from optimal control theory. Using only a few control parameters, we find that it is possible to implement one- and two-qubit gates on a system of spin-3/2 XXZ chains, such as Not, Hadamard, Pi-8, Phase, and C-Not, with fidelity levels exceeding 99%.

Our methods could easily be adapted to a variety of other systems.

## Acknowledgments

I would like to start by thanking my adviser Prof. Bruno Nachtergaele for his guidance during this thesis. I thank him for his remarkable intuition about mathematics and physics and his patience during the time when I was lacking it. I would also like to acknowledge my collaborators Shannon Starr, Robert Sims, Tom Michael all of whom I have learned so much from.

The faculty, students, post-docs and staff have combined to create a great academic atmosphere at UC Davis and I am proud to be a part of it for the last five years. All my teachers at UC Davis have been a tremendous inspiration to me and I would like to especially mention Prof. Craig Tracy, Prof. Roman Vershynin, Prof Greg Kuperberg and Prof. Alexander Soshnikov for serving as my role models in different ways.

I would like to thank all my teachers and mentors throughout my life who encouraged and cultivated my interest in science. Mrs. Dorothy, Father Tony Fonsceca and Mrs Alda from Holy Family High School, my friends at V.J.T.I., Prof Stuart Smith from California State University, Hayward, Shri A.V. Rajwade, Prof A.M. Dighe and Carl Sagan for creating the wonderful documentary *Cosmos* that first sparked my interest in science.

I thoroughly enjoyed having Davis as my home for five years. The Orchard Park graduate housing has been a safe and loving environment for my family and we will miss it. We also enjoyed the company and support of the Davis Indian community and the friends and relatives from the bay area, who often visited us in the bucolic surroundings of Davis and shared their joys with us.

My parents and my sister have always provided me their unconditional love and support, and their kindness constantly reminds me that being a good human being is even more important than being a good mathematician. My two sons Siddharth and Anand are a great source of joy and pride for me. It was a pleasure to come back from school to a smile on their faces. Finally I would like to thank my beautiful and talented wife Poonam for her courage to let me pursue my dreams. Without her this thesis would not have been possible.

## CHAPTER 1

**Introduction****1.1. Overview and motivation**

Quantum computing and quantum information theory harnesses the power of quantum mechanics to create a theoretical and practical framework for information processing and communication. It turns out that, at least in a few cases that have been discovered so far, there are some advantages of quantum computation over classical computation. A case in point is Shor's polynomial time factoring algorithm [Sho97], that is a great improvement on the best known classical algorithm for factoring, which takes exponential time. Even though there has been great progress in quantum computing and information theory in recent years it remains a great challenge to build a scalable quantum computer that will run the faster algorithms. The main hindrances to build a truly scalable physical implementation of quantum devices are the effects of noise and decoherence.

Quantum spin systems have been traditionally studied as models of magnetism. They have been successfully applied as statistical mechanical models to predict behaviours like phase transitions in a variety of physical systems. Spin systems are also very interesting from a purely mathematical perspective as they combine a variety of concepts drawn from analysis, representation theory, combinatorics etc. Quantum spin systems are also natural models for quantum computation. The focus of this thesis is the ferromagnetic XXZ spin model which is one of the best studied spin models that benefits from both analytic and algebraic techniques.

To build a quantum computer we first need to identify systems that are capable of running the faster algorithms and other information processing tasks. One of the primary requirements of any system suitable for quantum computing is the ability to encode qubits that are sufficiently decoupled from the environment and construct unitary gates on the space of qubits. There has been intensive research on finding systems that are most suited for quantum computing. Systems that have been investigated intensively are atomic levels

in ion traps [CZ95, MMK<sup>+</sup>95], superconducting device physics using Josephson rings [MOL<sup>+</sup>99], nuclear spins (using NMR in suitable molecules) [CVZ<sup>+</sup>98] and quantum dots [LD95].

Our focus in this thesis is the study of the ferromagnetic XXZ chain with a view of using some of its properties for quantum computation. We first study the low-lying spectrum of the XXZ chain with special boundary conditions and prove that the this model has interface states called ‘kinks’ that are isolated eigenstates of the Hamiltonian. While the presence of isolated eigenvalues in the one dimensional XXZ chain is interesting result in itself, it is also very good from the viewpoint of quantum computation since their isolated nature provides a natural protection from environmental noise. We then pursue an implementation scheme of constructing quantum gates on the subspace of these isolated eigenstates. Our results are a first step in the direction of using one-dimensional spin systems like the XXZ model, to encoded qubits and unitary gates.

## 1.2. Summary of results

The Hamiltonian of the one dimensional XXZ chain with spins on the integer lattice  $[-L, L]$  is given by

$$H_L^k(\Delta^{-1}) = \sum_{\alpha=-L}^{L-1} \left[ (J^2 - S_\alpha^3 S_{\alpha+1}^3) - \Delta^{-1} (S_\alpha^1 S_{\alpha+1}^1 + S_\alpha^2 S_{\alpha+1}^2) \right] + J\sqrt{1 - \Delta^{-2}} (S_{-L}^3 - S_L^3)$$

where  $S_\alpha^1, S_\alpha^2$  and  $S_\alpha^3$  are the spin  $J$  matrices acting on the site  $\alpha$ . The main parameter of the model is the anisotropy  $\Delta > 1$ , and the limit  $\Delta \rightarrow \infty$  is known as as the *Ising limit*. These boundary conditions lead to ground states with a domain wall between down spins on the left portion of the chain and up spins on the right. The XXZ kink Hamiltonian commutes with the operator  $S_{tot}^3 = \sum_{\alpha=-L}^L S_\alpha^3$ . We define  $\mathcal{H}_M$  to be the eigenspace of  $S_{tot}^3$  with eigenvalue  $M \in \{-J(2L+1), \dots, J(2L+1)\}$ . These subspaces are called ‘sectors’, and they are invariant subspaces for  $H_L^k(\Delta^{-1})$ . In [KNS01], Koma, Nachtergaele, and Starr showed that there is a spectral gap above each of the ground states in this model for all values of  $J$ . In chapter 3 we prove the existence of isolated eigenvalues in the low energy spectrum of the one dimensional Heisenberg ferromagnetic XXZ spin chain. Specifically, we have the following theorem

THEOREM 1.2.1 ([MNSS08]). *The spectrum of XXZ Hamiltonian with spin values  $J > \frac{3}{2}$  and  $\Delta > 18J^{5/2}$ , when restricted to any sector  $M$ , has isolated eigenvalues that persist in the thermodynamic limit.*

The main difficulty that we overcame was that in the thermodynamic limit, the perturbation of the entire chain is an unbounded operator, and therefore, the standard, finite-order perturbation theory was inadequate for a rigorous argument. The key idea was to prove that the XXZ model is a relatively bounded perturbation of the Ising limit.

In chapter 4 our goal is to construct quantum gates on the subspace corresponding to these isolated eigenvalues. The problem of constructing quantum gates can be described as a problem in quantum control theory. A primary goal in control theory is to drive a system via some external control parameters from an initial to a target state while minimizing (or maximizing) an objective function. We consider the problem of constructing quantum gates from the point of view of control theory. In our case our control system is the combined system of the XXZ spin chain and external control inputs coming from localized magnetic fields governed by the Schrödinger equation. Recently there have been many studies of controlling spin systems from the control viewpoint [D'A08]. Since analytic results to find optimal controls are known in cases of only 2 or 3 interacting spins [KBG01, DD01], in this thesis we follow a numerical approach. The main guiding principle in control theory is Pontryagin's maximum principle [Zab92] which provides necessary conditions for optimality of the control inputs. Our numerical method is based on a gradient based approach derived from the Pontryagin maximum principle as in [KRK<sup>+</sup>05]. To study the effects of the control inputs determined from optimal control theory on the XXZ chain, we use the Density Matrix Renormalization Group (DMRG) algorithm [Whi92]. DMRG is a quantum simulation method that has been very successfully applied to compute the static properties like ground state eigenvalues and correlation functions of strongly correlated quantum systems. It works by iteratively building the chain while also truncating the Hilbert space, thus choosing only the physically most relevant states. Recent modifications to this method has resulted in the development of a time dependent method that can be used to simulate the dynamic behaviour of the system [WF04]. We numerically simulate the XXZ chain by doing DMRG calculations that are adapted to the XXZ model. We have used optimal

control theory to determine the control fields to construct the quantum gates and then used the time dependent DMRG algorithm to simulate a single XXZ spin chain of up to 50 sites. Our results show the construction of several high fidelity elementary single qubit quantum gates and the two-qubit C-Not gate on the subspace of the isolated eigenvalues [MMN09].

We also have chapter 2 dedicated to give the reader the necessary background required to read the thesis. In sections 2.1 and 2.2 give some background on spin and quantum mechanics. We describe the XXZ model and review some important past results in section 2.3. In section 2.4 we introduce some important theorems on quantum gates and their efficient universal construction. Section 2.5 gives a brief description of control theory including the maximum principle and a gradient algorithm based on it. Finally, the DMRG algorithm and its adaptations to the XXZ model is presented in section 2.6. A reader who is well informed on these topics may skip to chapter 3 or 4.

In the appendix section we give the matlab code written for the control algorithm on the XXZ chain to obtain the gates. The DMRG code for the XXZ model was written by Tom Michoel and we adapted it to build quantum gates.

## CHAPTER 2

**Preliminaries****2.1. Spin**

The fundamental requirement in any quantum computation or quantum information set-up is a qubit. How do we know that such a structure exists in nature? The discovery of spin in 1922 provides the answer. Spin is a unique attribute of a quantum mechanical particle that has no classical equivalent. We describe the experiment that led to the discovery of spin known as the Stern-Gerlach experiment [Mes99, NC00]. In the classical view of an atom like hydrogen a charged electron is orbiting around a proton. According to electromagnetic theory the motion of a charge particle will induce a magnetic field and this will cause the particle to behave like a magnetic dipole. When this atom comes in contact with a magnetic field it causes it to be deflected. In the Stern-Gerlach experiment silver atoms were beamed from an oven into a magnetic field. This caused the atoms to be deflected and then measurements were made about the positions of the atoms. The experiment was set up in such a way that the atoms would be deflected depending on the  $z$  component of the magnetic moment of the atoms. Since the atoms coming out of the oven are expected to have their dipole moments distributed randomly in a uniform manner, it was expected that the observation of the  $z$  component would lead to a uniform and continuous distribution of angles. But surprisingly it was found that only a discrete set of peaks were observed. The conclusion of this experiment was that electrons had an intrinsic angular momentum component that was not related to its orbital motion around the nucleus which was quantized i.e. had a discrete set of observable values. After a lot of experimentation and mathematical analysis the spin was put into a mathematical framework of quantum mechanics that we describe in the next section.

## 2.2. Quantum Mechanics

Quantum mechanics provides a mathematical framework to describe physical theories of the small scale i.e. atomic and sub-atomic phenomenon. In this section we give a brief description of quantum mechanics from the viewpoint of the basic postulates and mathematical tools that are necessary for us in this thesis. Quantum mechanics of course is a vast subject and an excellent comprehensive view can be found in [Mes99]. In quantum mechanics the state of a system is identified with an element of a Hilbert space  $\mathcal{H}$ . In the Bra-ket notation as introduced by Dirac a *ket* vector  $|\phi\rangle$  is an element of the Hilbert space and its dual vector *bra* written as  $\langle\psi|$  is a continuous linear functional  $\langle\psi| : \mathcal{H} \rightarrow \mathbb{C}$ . The dual vector  $\langle\psi|$  acts on  $|\phi\rangle$  as  $\langle\psi|(|\phi\rangle) = \langle\psi|\phi\rangle$  where  $\langle\cdot|\cdot\rangle$  is the inner product defined on the Hilbert space. The postulates of quantum mechanics are as follows:

- (1) Associated with each physical system is a Hilbert space. The state of a quantum mechanical particle is a normalized vector in this Hilbert space. For example the state of a spin  $\frac{1}{2}$  is a normalized vector in the complex Hilbert space  $\mathbb{C}^2$ . In this case the state  $|\psi\rangle$  may be represented in some basis  $|0\rangle$  and  $|1\rangle$  as

$$|\psi\rangle = a|0\rangle + b|1\rangle \quad a, b \in \mathbb{C}$$

with  $|a|^2 + |b|^2 = 1$ . A state space of a spin  $\frac{1}{2}$  particle, or for that matter any space that is isomorphic to  $\mathbb{C}^2$ , is a qubit.

- (2) Associated with a physical quantity (say position, momentum, spin in the x-direction) that can be measured, are Hermitian operators on the state space called ‘Observables’. A Hermitian operator (finite dimensional) has the spectral decomposition  $A = \sum_m \lambda_m A_m$  where  $A_m$  is the projection onto the eigenspace corresponding to eigenvalue  $\lambda_m$ . Given an initial state  $|\psi_0\rangle$  a ‘measurement’ results in getting observed values that are eigenvalues of the observable  $A$ . The probability of getting an observed value of  $\lambda_m$  is obtained by projecting  $|\psi_0\rangle$  onto the eigenspace of  $\lambda_m$

$$P_{\lambda_m} = \langle\psi_0|A_m\psi_0\rangle = Tr(A_m|\psi_0\rangle\langle\psi_0|)$$

In general, a measurement of the state that results the observed value  $\lambda_m$ , modifies the state and the post-measurement state is given by

$$|\psi_m\rangle = \frac{A_m|\psi_0\rangle}{\|A_m|\psi_0\rangle\|} = \frac{A_m|\psi_0\rangle}{\sqrt{P_{\lambda_m}}}$$

Given an initial state  $|\psi_0\rangle$  the expectation value of the observable  $A$  is thus given by

$$\begin{aligned}\omega(A) &= \sum_m \lambda_m P_{\lambda_m} \\ &= \sum_m \lambda_m \langle \psi_0 | A_m \psi_0 \rangle \\ &= \langle \psi_0 | \sum_m \lambda_m A_m \psi_0 \rangle \\ &= \langle \psi_0 | A \psi_0 \rangle = \text{Tr}(|\psi_0\rangle\langle\psi_0| A)\end{aligned}$$

Let us take a very elementary example, the observation of a spin  $\frac{1}{2}$  particle in the z-direction. The  $S^3$  observable has a spectral decomposition

$$S^3 = \frac{1}{2} \left| \frac{1}{2} \right\rangle \left\langle \frac{1}{2} \right| - \frac{1}{2} \left| -\frac{1}{2} \right\rangle \left\langle -\frac{1}{2} \right|$$

If the initial state is

$$|\psi_0\rangle = a \left| \frac{1}{2} \right\rangle + b \left| -\frac{1}{2} \right\rangle$$

then observing the spin  $\frac{1}{2}$  particle results in getting the observed value  $\frac{1}{2}$  with probability

$$P_{\frac{1}{2}} = \left\langle \psi_0 \left| \frac{1}{2} \right\rangle \left\langle \frac{1}{2} \right| \psi_0 \right\rangle = |a|^2$$

and the post measurement state is

$$|\psi_{\frac{1}{2}}\rangle = \frac{\left| \frac{1}{2} \right\rangle \left\langle \frac{1}{2} \right| \psi_0}{\sqrt{P_{\frac{1}{2}}}} = \frac{a}{|a|} \left| \frac{1}{2} \right\rangle$$

One can see that an initial state of  $e^{i\theta}|\psi_0\rangle$  instead of  $|\psi_0\rangle$  results in the same  $P_{\lambda_m}$  and  $|\psi_m\rangle$  and hence a phase difference in initial states do not result in any observable differences.

- (3) The time evolution of a closed quantum (isolated from the environment) is given by the Schrödinger equation

$$|\dot{\psi}(t)\rangle = -iH|\psi(t)\rangle$$

Here  $H$  is Hamiltonian which is the observable corresponding to the total energy of the system. If  $H$  is not time dependent then the solution of this differential equation is just

$$|\psi(t)\rangle = e^{-iHt}|\psi_0\rangle$$

It is easy to see that the evolution operator  $U(t) = e^{-iHt}$  also obeys

$$(2.1) \quad \dot{U}(t) = -iHU(t)$$

with initial condition  $U(0) = \mathbb{1}$ .

- (4) The state space of a composite system the tensor product of the state space of the two subsystems. Thus the state space of two spin half particles isolated from the environment is  $\mathbb{C}^2 \otimes \mathbb{C}^2$ . If we have two non interacting quantum systems each with Hilbert spaces  $\mathcal{H}_1$  and  $\mathcal{H}_2$  and Hamiltonian's  $H_1$  and  $H_2$  respectively and an initial state of  $|\psi_0^{(1)}\rangle \otimes |\psi_0^{(2)}\rangle$  then according to postulate (3) the state after time  $t$  will be  $e^{-iH_1t}|\psi_0^{(1)}\rangle \otimes e^{-iH_2t}|\psi_0^{(2)}\rangle$ . It is easy to check that a general state  $|\psi_0^{(1,2)}\rangle$  of the state space  $\mathcal{H}_1 \otimes \mathcal{H}_2$  of such a non-interacting composite system thus evolves under the effective Hamiltonian  $H_1 \otimes \mathbb{1}_2 + \mathbb{1}_1 \otimes H_2$

The state vector described in postulate (1) is an example of a *pure state*. In general the state of a quantum system may be an ensemble of pure states. More precisely the state can be in one of the pure quantum states  $|\psi_i\rangle$  with probability  $p_i$ . An *ensemble*  $\{p_i, |\psi_i\rangle\}$  where  $\sum_i p_i = 1$  is called a *mixed* state and can be represented by a density matrix

$$\rho = \sum_i p_i |\psi_i\rangle \langle \psi_i|$$

Of course if the state is pure with state vector  $|\psi\rangle$  its density matrix is given by the one dimensional projection  $\rho = |\psi\rangle \langle \psi|$ . Any density operator satisfies the trace condition  $Tr(\rho) = 1$  and also the positivity condition  $\rho \geq 0$ . Conversely it can also be shown that for any operator that satisfies the trace and positivity condition there is an ensemble that

represents a mixed state. The time evolution of a density matrix is governed by the following equation

$$\dot{\rho}(t) = -i[H, \rho(t)]$$

The expectation value of an observable  $M$  given the initial mixed state  $\rho$  is

$$\omega(A) = \text{Tr}(\rho M)$$

Suppose we have a mixed state given by the density matrix  $\rho^{AB}$  on the composite Hilbert space  $\mathcal{H}_A \otimes \mathcal{H}_B$  then one can ask the question: what is the state with respect to the subsystem  $\mathcal{H}_A$ ? More precisely, given any observable  $M_A$  that acts only on  $\mathcal{H}_A$  is there a state  $\rho^A$  of the subsystem  $\mathcal{H}_A$  such that an observation performed on this state with  $M_A$  gives the same measurement statistic as the same observation performed on  $\rho^{AB}$ ? The answer to this question is in the affirmative, in fact there is a unique state such that

$$\text{Tr}(\rho^{AB}(M_A \otimes \mathbb{I}_B)) = \text{Tr}(\rho^A M_A)$$

The state  $\rho^A$  is called the *reduced density matrix* of  $\rho^{AB}$ . A very interesting thing is, that the reduced density matrix of a pure state can be a mixed state. For example one can easily show that suppose one has a two qubit system that is in the state *Bell state*  $\frac{|00\rangle + |11\rangle}{\sqrt{2}}$  then the reduced density matrix of the first(second) qubit is the *maximally mixed* state  $\mathbb{I}/2$ .

In a bipartite system  $\mathcal{H}_A \otimes \mathcal{H}_B$  there can be states that are *entangled*. Entanglement has emerged as one of the most powerful concepts especially from the view point of quantum computation and quantum information theory. Entanglement is an essential resource that is believed to be responsible for the superiority of quantum algorithms and quantum communication protocols. In broad terms entanglement describes correlations between observables. Entanglement is a topic that could easily fill a whole thesis and we point to [HHHH07] for further reading. Our interest in this thesis in entanglement is its connection with the efficiency of the DMRG procedure which we will describe in section 2.6. A pure state  $|\psi_{AB}\rangle$  of a bi-partite system is *separable* if it can be written as a simple tensor  $|\psi_A\rangle \otimes |\psi_B\rangle$ , otherwise it is entangled. It is important to quantify entanglement and the following theorem gives us a way to put a measure of entanglement when the state is pure

THEOREM 2.2.1. (*Schmidt Decomposition*) If  $|\psi\rangle$  is a pure state of a bi-partite system  $\mathcal{H}_A \otimes \mathcal{H}_B$  then there exist orthonormal sets  $\{|i_A\rangle\}$  and  $\{|i_B\rangle\}$

$$|\psi_{AB}\rangle = \sum_i \lambda_i |i_A\rangle |i_B\rangle \quad \lambda_i > 0, \quad \sum_i \lambda_i^2 = 1;$$

Given such a decomposition of a pure state it is possible it is easy to see that the reduced density matrices are given by

$$\begin{aligned} \rho^A &= \sum_i \lambda_i^2 |i_A\rangle \langle i_A| \\ \rho^B &= \sum_i \lambda_i^2 |i_B\rangle \langle i_B| \quad \sum_i \lambda_i^2 = 1 \end{aligned}$$

The Schmidt vectors  $\{|i_A\rangle\}$  and  $\{|i_B\rangle\}$  are thus the eigenvectors of the reduced density matrices  $\rho^A$  and  $\rho^B$ . The rank of these reduced density matrices called the *Schmidt Rank*. Using the Schmidt decomposition of a state one can obtain a measure of entanglement of this state between the two subsystems. The measure is known as *Entropy of Entanglement* and is given by

$$E(\psi_{AB}) := S(\rho^A) = - \sum_i \lambda_i^2 \log_2 \lambda_i^2$$

One can see that when a state is a product state i.e.  $|\psi_{AB}\rangle = |\psi_A\rangle \otimes |\psi_B\rangle$  then this measure is zero. On the other hand this measure is maximized on what are known as *maximally entangled states*. They are states of the form

$$\frac{|0,0\rangle + |1,1\rangle + \cdots + |d,d\rangle}{\sqrt{d}}$$

where  $d$  is the dimension of each subsystem. It is an easy calculation to verify that the *Entropy of Entanglement* in the case of a maximally entangled state is equal to  $\log(d)$ .

### 2.3. XXZ Model

Spin models were first proposed as a mathematical model of magnetism. In this models atoms or ions are arranged on a lattice  $\Lambda$  which typically is a subset of  $\mathbb{Z}^d$  where  $d = 1, 2, 3$  typically. At each site  $\alpha$  the atoms or ions have the spin property with spin values  $J_\alpha = \{\frac{1}{2}, 1, \frac{3}{2}, \dots\}$ . The Hilbert space at each single site  $\alpha \in \Lambda$  is  $\mathcal{H}_\alpha = \mathbb{C}^{2J_\alpha+1}$  and for the entire spin system is  $\mathcal{H}_\Lambda = \otimes_{\alpha \in \Lambda} \mathcal{H}_\alpha$ . At each site the Hilbert space  $\mathcal{H}_\alpha$  also carries the action of

the matrix Lie group  $SU(2)$  [Hal04]. This induces an action ( $2J+1$  dimensional irreducible representation) of the Lie algebra algebra  $\mathfrak{su}(2)$ , which is a vector space over  $\mathbb{R}$  of Hermitian matrices with trace zero. The important operators at each site are  $S_\alpha^1, S_\alpha^2$  and  $S_\alpha^3$  that are the generators of the  $2J+1$  dimensional irreducible representation of  $\mathfrak{su}(2)$  denoted by  $\mathcal{D}^{(J_\alpha)}$ . They represent the observables that correspond to measuring the spin in the x,y and z directions respectively. The  $S_\alpha^3$  operator has  $2J+1$  eigenvalues  $J, J-1, \dots, -J$  with respective eigenvectors  $|J\rangle, |J-1\rangle, \dots, |-J\rangle$ . The  $2J+1$  eigenvalues of these observables are the measured values of the spin in that direction. Thus we have

$$S_\alpha^3|m_\alpha\rangle = m_\alpha|m_\alpha\rangle$$

One can show that if we define the two raising and lowering operators

$$S_\alpha^\pm = S_\alpha^1 \pm iS_\alpha^2$$

then we have the following relations

$$S^+|m_\alpha\rangle = \begin{cases} \sqrt{J(J+1) - m_\alpha(m_\alpha+1)}|m_\alpha+1\rangle & \text{if } -J \leq m_\alpha \leq J-1 \\ 0 & \text{if } m_\alpha = J \end{cases}$$

$$S^-|m_\alpha\rangle = \begin{cases} \sqrt{J(J+1) - m_\alpha(m_\alpha-1)}|m_\alpha-1\rangle & \text{if } -J+1 \leq m_\alpha \leq J \\ 0 & \text{if } m_\alpha = -J \end{cases}$$

Using these relations one can explicitly write down the spin matrices. For example the spin  $\frac{1}{2}$  particles these observables are given by

$$S^1 = \frac{1}{2} \begin{pmatrix} 0 & 1 \\ 1 & 0 \end{pmatrix}, S^2 = \frac{1}{2} \begin{pmatrix} 0 & -i \\ i & 0 \end{pmatrix}, S^3 = \frac{1}{2} \begin{pmatrix} 0 & -i \\ i & 0 \end{pmatrix}$$

respectively. They obey the following commutation relation.

$$[S^a, S^b] = i\epsilon_{abc}S^c$$

where  $\epsilon_{abc}$  is the Levi-Civita symbol. For spin 1 the matrices are

$$S^1 = \frac{1}{\sqrt{2}} \begin{pmatrix} 0 & 1 & 0 \\ 1 & 0 & 1 \\ 0 & 1 & 0 \end{pmatrix}, S^2 = \frac{1}{\sqrt{2}} \begin{pmatrix} 0 & -i & 0 \\ i & 0 & -i \\ 0 & i & 0 \end{pmatrix}, S^3 = \begin{pmatrix} 1 & 0 & 0 \\ 0 & 0 & 0 \\ 0 & 0 & -1 \end{pmatrix}$$

One of the first quantum models that was proposed as a model for magnetism was the Heisenberg model. The Hamiltonian of this model representing atoms on a lattice site  $\Lambda$  with nearest neighbor interactions is given by

$$(2.2) \quad H = - \sum_{\substack{\{\alpha, \beta\} \subset \Lambda \\ |\alpha - \beta| = 1}} J(\alpha, \beta) \mathbf{S}_\alpha \cdot \mathbf{S}_\beta$$

where we define the spin vector  $\mathbf{S}_\alpha = (S_\alpha^1, S_\alpha^2, S_\alpha^3)$ . The  $J(\alpha, \beta)$  are coupling constants that are assumed to be positive. This is an example of a ferromagnetic interaction because of the overall  $-1$  in front of the sum. Ferromagnetism involves a phenomenon where neighboring spins tend to align spontaneously without any applied field. An important feature of the Hamiltonian 2.2 is that it commutes with the entire representation  $\otimes_{\alpha \in \Lambda} \mathcal{D}^{(J_\alpha)}$  of  $SU(2)$ . In particular it commutes with the total spin matrices

$$S_\Lambda^i = \sum_{\alpha \in \Lambda} S_\alpha^i \quad i = 1, 2, 3$$

and hence also with the Casimir operator

$$C = \mathbf{S}_\Lambda \cdot \mathbf{S}_\Lambda$$

The eigenvalues of  $C$  are  $J(J+1)$  with  $J$  ranging between  $J_{min}, J_{min} + 1, \dots, J_{max} = \sum_{\alpha \in \Lambda} J_\alpha$ . These are the spin labels that occur in the decomposition of a tensor product of irreducible representations as a direct sum of its irreducible components. These are given by the Clebsch-Gordan series.

$$\mathcal{D}^{(J_1)} \otimes \mathcal{D}^{(J_2)} = \mathcal{D}^{(J_1+J_2)} \oplus \dots \oplus \mathcal{D}^{(|J_1-J_2|)}$$

A more general form of the spin model is the XYZ model with an exchange of the form

$$J_1 S_\alpha^1 S_\beta^1 + J_2 S_\alpha^2 S_\beta^2 + J_3 S_\alpha^3 S_\beta^3$$

with  $J_1 \neq J_2 \neq J_3$ . If we set all the coupling constants  $J(\alpha, \beta)$  to a constant then we get an isotropic exchange or the XXX model. This is a relatively simpler model to study. Since most materials do have an anisotropic exchange a relevant model to study is when  $J_1 = J_2$  and  $J_3 = 1$  and hence is called the XXZ model. We will study this model in this thesis with ‘kink’ boundary terms. An excellent reference for the XXZ model and its properties is [Sta01]. The Hamiltonian of the model we will be studying is given by

$$H_L^k(\Delta^{-1}) = \sum_{\alpha=-L}^{L-1} \left[ (J^2 - S_\alpha^3 S_{\alpha+1}^3) - \Delta^{-1} (S_\alpha^1 S_{\alpha+1}^1 + S_\alpha^2 S_{\alpha+1}^2) \right] + J \sqrt{1 - \Delta^{-2}} (S_{-L}^3 - S_L^3)$$

where  $S_\alpha^1, S_\alpha^2$  and  $S_\alpha^3$  are the spin  $J$  matrices acting on the site  $\alpha$ . Apart from the magnitude of the spins,  $J$ , the main parameter of the model is the anisotropy  $\Delta > 1$  and we will refer to the limit  $\Delta \rightarrow \infty$  as the *Ising limit*. In the case of  $J = 1/2$  these boundary conditions were first introduced in [PS90]. They lead to ground states with a domain wall between down spins on the left portion of the chain and up spins on the right. The domain wall is exponentially localized. The third component of the magnetization,  $M$ , is conserved, and there is exactly one ground state for each value of  $M$ . Different values of  $M$  correspond to different positions of the domain walls, which in one dimension are sometimes referred to as kinks. In [ASW95] and [GW96] the ground states for this type boundary conditions were further analyzed and generalized to higher spin,  $J$ . The XXZ kink Hamiltonian commutes with the operator  $S_{tot}^3 = \sum_{\alpha=-L}^L S_\alpha^3$ . We define  $\mathcal{H}_M$  to be the eigenspace of  $S_{tot}^3$  with eigenvalue  $M \in \{-J(2L+1), \dots, J(2L+1)\}$ . These subspaces are called ‘sectors’, and they are invariant subspaces for  $H_L^k(\Delta^{-1})$ .

It was shown in [ASW95, GW96, Mat95, KN98] that for each sector there is a unique ground state of  $H_L^k(\Delta^{-1})$  with eigenvalue 0. Moreover, this ground state,  $\psi_M$ , is given by the following expression:

$$\psi_M = \sum_{\alpha \in [-L, L]} \bigotimes_{\alpha \in [-L, L]} \binom{2J}{J - m_\alpha}^{1/2} q^{\alpha(J - m_\alpha)} |m_\alpha\rangle_\alpha,$$

where the sum is over all configurations for which  $\sum_\alpha m_\alpha = M$  and the relationship between  $\Delta > 1$  and  $q \in (0, 1)$  is given by  $\Delta = (q + q^{-1})/2$ . An easy calculation shows a sharp transition in the magnetization from fully polarized down at the left to fully polarized up at the right. For this reason they are called kink ground states. In [KN98] Koma and

Nachtergaele proved that the kink ground states (as well as their spin-flipped or reflected versions the antikinks) comprise the entire set of ground states for the infinite-volume model, aside from the 2 other ground states: the translation invariant maximally magnetized and minimally magnetized all  $+J$  and all  $-J$  groundstates.

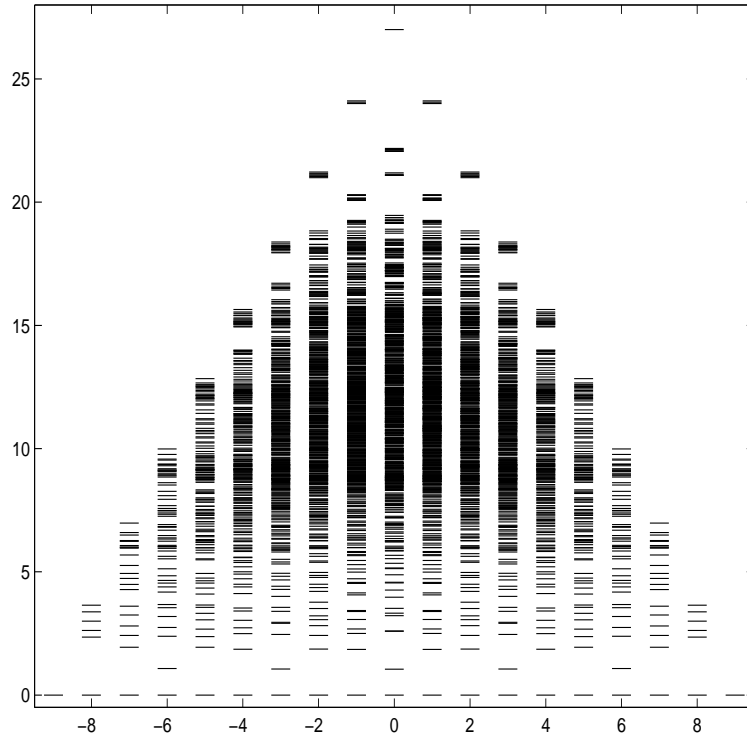


FIGURE 2.1. The Spectrum of the XXZ Model with kink boundary conditions for  $J = 3/2$  and  $L=6$  and  $\Delta^{-1} = 0.3$ .

In [KNS01], Koma, Nachtergaele, and Starr showed that there is a spectral gap above each of the ground states in this model for all values of  $J$ . The figure 2.1 shows the spectrum of an XXZ chain of length 6. Based on numerical evidence, they also made a conjecture that for  $J \geq \frac{3}{2}$  the first excited state of the XXZ model is an isolated eigenvalue, and that the magnitude of the spectral gap is asymptotically given by  $J\gamma(\Delta)$ , where  $\gamma(\Delta)$  is an eigenvalue of a particular one-particle problem. Caputo and Martinelli [CM03] showed that the gap is indeed of order  $J$ . In chapter 3 we show that for sufficiently large  $\Delta$  the first few excitations of the XXZ Hamiltonian when restricted to a sector are isolated eigenvalues.

### 2.4. Quantum gates

A quantum gate represents evolution of a qubit, governed by the Schrödinger's equation.

$$|\dot{\psi}\rangle = -iH|\psi\rangle$$

The figure 2.2 shows some examples of quantum gates with their matrix representations and their action on qubits.

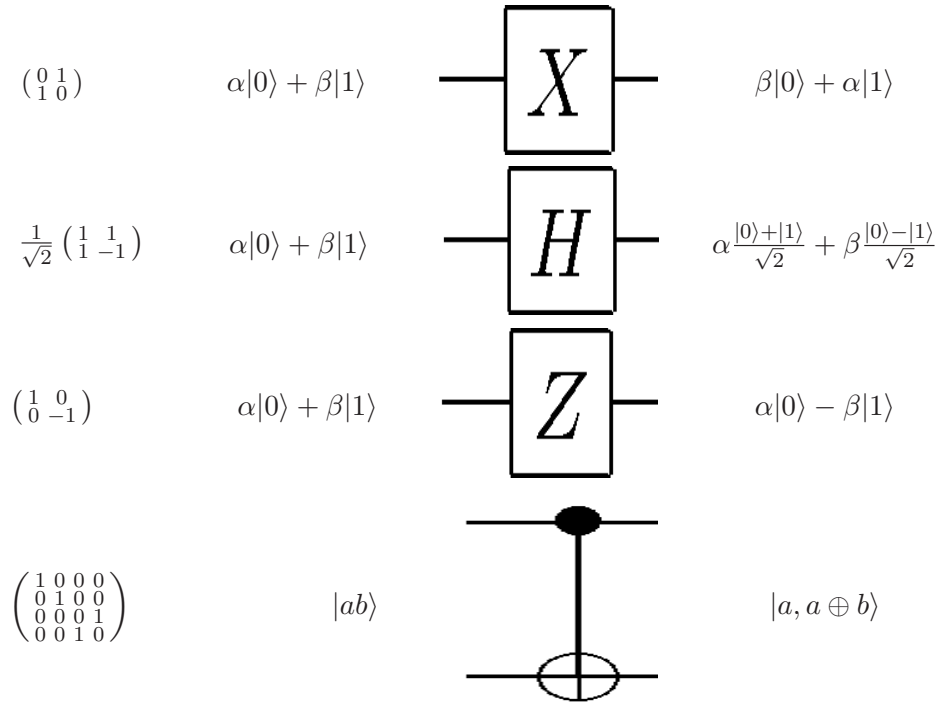


FIGURE 2.2. The action of the Not(X), Hadamard(H)and Z single qubit gates and the two-qubit C-Not gate.

An arbitrary qubit  $|\psi\rangle$  can be visualized as a point  $(\theta, \phi)$  on a unit sphere called Bloch sphere as shown in figure 2.3 with  $|\psi\rangle = \cos(\frac{\theta}{2})|0\rangle + e^{i\phi} \sin(\frac{\theta}{2})|1\rangle$ .

We define

$$R_{\vec{n}}(\theta) := e^{-i\frac{\theta}{2}\vec{n}\cdot\vec{\sigma}}$$

where  $\vec{\sigma} = (\sigma^1, \sigma^2, \sigma^3)$  are the Pauli matrices and  $\vec{n}$  is a unit vector in  $\mathbb{R}^3$ , then one can show that  $R_{\vec{n}}(\theta)$  is a rotation by an angle  $0 \leq \theta < 2\pi$  about the  $\vec{n}$  axis of the Bloch sphere and we have the following two lemmas.

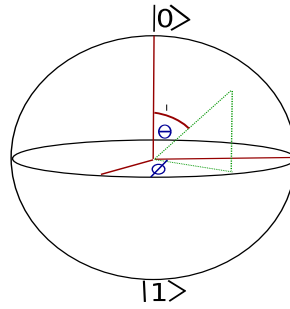


FIGURE 2.3. The Bloch Sphere

LEMMA 2.4.1 ([NC00]). *Any arbitrary single qubit quantum gate can be written as  $e^{i\alpha}R_{\vec{n}}(\theta)$  for some  $\alpha, \theta \in \mathbb{R}$  and for some unit vector  $\vec{n}$  in  $\mathbb{R}^3$ .*

LEMMA 2.4.2 ([NC00]). *Suppose  $\vec{m}$  and  $\vec{n}$  are two non parallel unit vectors in three dimensions then any arbitrary single qubit Unitary  $U$  may be written as*

$$U = e^{i\alpha}R_{\vec{n}}(\beta)R_{\vec{m}}(\gamma)R_{\vec{n}}(\delta)$$

for some  $\alpha, \beta, \gamma$  and  $\delta \in \mathbb{R}$ .

Two important questions about quantum gates are the questions of universality and efficiency. Is there a universal discrete set of quantum gates? In other words is there a small set of single qubit gates such that arbitrary long words made out of this set produce all other gates to arbitrary accuracy? First let us answer this question for single qubit gates. Since any single qubit gate is up to a phase factor is an element of  $SU(2)$  we need a set that will generate a dense subset of  $SU(2)$ . We have the following theorem.

THEOREM 2.4.3 ([NC00]). *The Hadamard( $H$ ), Not( $X$ ), Pi-8 ( $S$ ) and Phase( $T$ ) gates are universal for single qubit quantum computation.*

We give a rough idea of the proof. Using this discrete set one generates a rotation of an irrational multiple of  $\pi$  about two non parallel axes of the Bloch sphere. Hence one can generate a rotation of any arbitrary angle to required accuracy by applying a sufficiently long sequence of this discrete set about these two specific axes. Then using lemmas 2.4.1 and 2.4.2 we can get an any arbitrary gate.

In fact such a construction of any gate can be made efficient. The following theorem known as Solovay-Kitaev theorem says that this is possible.

THEOREM 2.4.4 (Solovay-Kitaev [NC00]). Let  $\mathcal{G}$  be a discrete set of Universal gates.  $\langle \mathcal{G}_l \rangle$  be all words of length at most  $l$  and  $\langle \mathcal{G} \rangle$  be all words of finite length such that  $\overline{\langle \mathcal{G} \rangle} = SU(2)$ . Given an arbitrary  $U \in SU(2)$  and  $\epsilon > 0$  one can approximate  $U$  to within  $\epsilon$  by  $\langle \mathcal{G}_l \rangle$  for  $l = O(\log^c(\frac{1}{\epsilon}))$  where  $c \approx 2$ .

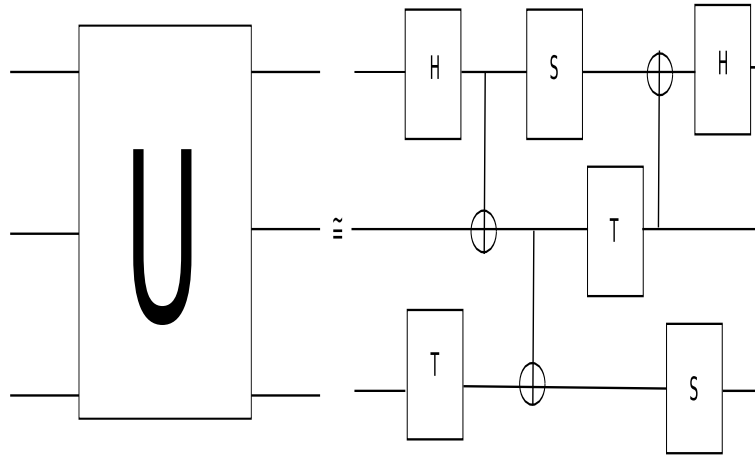


FIGURE 2.4. Universal construction of n-qubit unitaries can be done using the universal single qubit set (Hadamard (H), Phase (T) and Pi-8(S)) and C-Not gates.

The following theorem says that a universal construction of n-qubit quantum gates can be done using a universal set of single qubit gates and C-Not gates. (see also figure 2.4)

THEOREM 2.4.5 ([NC00]). A set of universal single qubit gates and nearest neighbor C-Not gates is universal for n-qubit quantum computation.

## 2.5. Optimal Control Theory

The objective of optimal control theory is to design control inputs that satisfy the physical constraints and at the same time optimize a certain performance measure. A control system can be modelled using differential equations using the *state variable* approach [Zab92, Kir04]. If  $x_1(t), \dots, x_n(t)$  are the states of the process at time  $t$  and  $u_1(t), \dots, u_m(t)$

are the control inputs then the system may be described by  $n$  first order differential equations

$$\begin{aligned}\dot{x}_1(t) &= f_1(x_1(t), \dots, x_n(t), u_1(t), \dots, u_m(t), t) \\ \dot{x}_2(t) &= f_2(x_1(t), \dots, x_n(t), u_1(t), \dots, u_m(t), t) \\ &\vdots \\ \dot{x}_n(t) &= f_n(x_1(t), \dots, x_n(t), u_1(t), \dots, u_m(t), t)\end{aligned}$$

We define

$$\mathbf{x}(t) := \begin{bmatrix} x_1(t) \\ \vdots \\ x_n(t) \end{bmatrix}$$

to be the state vector at time  $t$  and

$$\mathbf{u}(t) := \begin{bmatrix} u_1(t) \\ \vdots \\ u_m(t) \end{bmatrix}$$

to be the control vector at time  $t$  and our control system is defined as the dynamical constraint

$$(2.3) \quad \dot{\mathbf{x}} = \mathbf{f}(\mathbf{x}, \mathbf{u}, t) \quad \mathbf{x} : \mathbb{R} \rightarrow \mathbb{R}^n, \mathbf{u} : \mathbb{R} \rightarrow \mathbb{R}^m$$

In many physical situations there are constraints on the control and state functions may belong to an *admissible* set  $\mathbf{u} \in \mathcal{U}$  and  $\mathbf{x} \in \mathcal{X}$ . State and control functions that satisfy these constraints are called admissible trajectories and admissible controls. A general form of a performance measure is the cost functional  $J : \mathcal{U} \rightarrow \mathbb{R}$  given by

$$(2.4) \quad J(\mathbf{u}) := h(\mathbf{x}(T), T) + \int_0^T L(\mathbf{x}, \mathbf{u}, t) dt$$

Typical costs are as follows:

- (1) Minimizing time:  $J(\mathbf{u}) = T$
- (2) Minimizing Energy:  $J(\mathbf{u}) = \int_0^T \|\mathbf{u}(t)\|^2 dt$
- (3) Minimizing distance from end state:  $J(\mathbf{u}) = \|\mathbf{x}(T) - \mathbf{x}_f\|^2$

$$(4) \text{ Tracking: } J(\mathbf{u}) = \int_0^T \|\mathbf{x}(t) - \mathbf{r}(t)\|^2 dt$$

An admissible control  $\mathbf{u}^*$  that causes the system 2.3 to follow an admissible trajectory  $\mathbf{x}^*$  that minimizes the performance measure 2.4 is called an *optimal control*. A control system is said to be *completely controllable* if we can reach all states from any given initial state using a set of admissible controls. Given a control system and an objective function to maximize (or minimize) how do we find optimal controls? Optimal control theory was invented as a generalization of calculus of variations by the Russian mathematician Pontryagin and his co-workers. We first remind the reader of the following definitions.

DEFINITION 2.5.1. *If  $\mathbf{x}$  and  $\mathbf{x} + \delta\mathbf{x}$  are functions for which the functional  $J$  is defined then the increment of  $J$ , denoted by  $\Delta J$  is*

$$\Delta J = J(\mathbf{x} + \delta\mathbf{x}) - J(\mathbf{x})$$

The increment of a functional can be written as

$$\Delta J(\mathbf{x}, \delta\mathbf{x}) = \delta J(\mathbf{x}, \delta\mathbf{x}) + g(\mathbf{x}, \delta\mathbf{x}) \cdot \|\delta\mathbf{x}\|$$

where  $\delta J$  is linear in  $\delta\mathbf{x}$ .

DEFINITION 2.5.2. *If  $\lim_{\|\delta\mathbf{x}\| \rightarrow 0} g(\mathbf{x}, \delta\mathbf{x}) = 0$  then  $J$  is said to be differentiable on  $\mathbf{x}$  and  $\delta J$  is the variation of  $J$  evaluated for the function  $\mathbf{x}$ .*

DEFINITION 2.5.3. *A functional  $J$  with domain  $\Omega$  has a relative extremum at  $\mathbf{x}^*$  if there exists an  $\epsilon > 0$  such that for all functions in  $\Omega$  that satisfy  $\|\mathbf{x} - \mathbf{x}^*\| < \epsilon$  the increment of  $J$  has the same sign. If  $\Delta J = J(\mathbf{x}) - J(\mathbf{x}^*) \geq 0$  then  $J(\mathbf{x}^*)$  is a relative minimum. If  $\Delta J = J(\mathbf{x}) - J(\mathbf{x}^*) \leq 0$  then  $J(\mathbf{x}^*)$  is a relative maximum.  $\mathbf{x}^*$  is called extremal and  $J(\mathbf{x}^*)$  is referred to as extremum.*

The fundamental theorem of calculus of variations is

THEOREM 2.5.4. *If  $\mathbf{x}^*$  is an extremal for a differentiable functional  $J$  then  $\delta J(\mathbf{x}^*, \delta\mathbf{x}) = 0$  for all admissible  $\delta\mathbf{x}$ .*

In typical calculus of variations problem the fundamental theorem is applied to a functional of the form

$$J(\mathbf{x}) = \int_{t_0}^{t_1} \mathbf{g}(\mathbf{x}, \dot{\mathbf{x}}, t) dt$$

to obtain the Euler-Lagrange equations. If  $\mathbf{x}^*$  is an extremal for the functional  $J(x)$  then

$$\frac{\partial \mathbf{g}}{\partial \mathbf{x}}(\mathbf{x}^*(t), \dot{\mathbf{x}}^*(t), t) - \frac{d}{dt} \left[ \frac{\partial \mathbf{g}}{\partial \dot{\mathbf{x}}}(\mathbf{x}^*, \dot{\mathbf{x}}^*, t) \right] = 0$$

In calculus of variations problems there is no external forcing function or control input. The Pontryagin maximum principle generalizes the Euler-Lagrange equations in a system with an external forcing input as in equation 2.3 with costs described with equation 2.4. We state a special case of the maximum principle theorem when the performance measure to be minimized is the distance from the end state  $J(\mathbf{u}) = \|\mathbf{x}(T) - \mathbf{x}_f\|$  and when there is no a-priori bound on the controls.

**THEOREM 2.5.5** (Pontryagin maximum principle). *If  $\mathbf{u}^*$  are optimal controls for the control system 2.3 with optimal trajectory  $\mathbf{x}^*$  then there exists a Lagrange multiplier  $\lambda(t)$  and a Hamiltonian function defined by*

$$\mathcal{H} := \lambda'(t)[\mathbf{f}(\mathbf{x}(t), \mathbf{u}(t), t)]$$

*The Lagrange multiplier follows the following costate trajectory*

$$(2.5) \quad \dot{\lambda}(t) = \frac{\partial \mathcal{H}}{\partial \mathbf{x}}(\mathbf{x}^*(t), \mathbf{u}^*(t), \lambda(t), t)$$

*satisfying the terminal conditions*

$$(2.6) \quad \lambda(T) = \frac{\partial h}{\partial \mathbf{x}}(\mathbf{x}^*(T), T)$$

*such that*

$$(2.7) \quad \frac{\partial \mathcal{H}}{\partial \mathbf{u}}(\mathbf{x}^*(t), \mathbf{u}^*(t), \lambda(t), t) = 0$$

*for all  $t \in [0, T]$ .*

We clarify that the Hamiltonian function referred in the principle is different from the quantum mechanical Hamiltonian. For a proof of this theorem we refer the reader to [Kir04]. The maximum principle readily lends itself to a gradient based algorithm (see

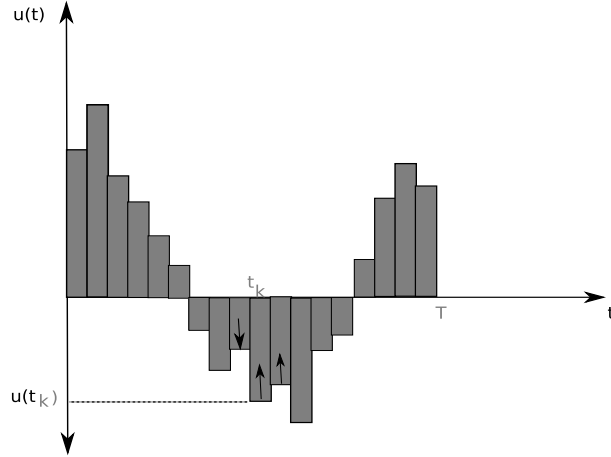


FIGURE 2.5. Gradient based algorithm based on the Pontryagin's maximum principle. The arrows indicate the direction of the gradient and the controls in the next iteration are adjusted in the direction of the arrows.

figure 2.5) to compute optimal controls. This can be described as follows

- (1) Select a an initial discrete approximation to the control  $\mathbf{u}(t)$ . This can be done by dividing the interval  $[0, T]$  into  $N$  sub intervals and considering the control  $\mathbf{u}^{(0)}$  as being piecewise constant on these sub intervals.

$$\mathbf{u}^{(0)}(t) = \mathbf{u}^{(0)}(t_k) \quad t \in [t_k, t_{k+1}], k = 0, \dots, N - 1$$

The piecewise constant control  $\mathbf{u}^{(0)}$  is stored in the computers memory. Start from an iteration index  $i = 0$ .

- (2) Use the control  $\mathbf{u}^i$  and the initial condition  $\mathbf{x}(0) = \mathbf{x}_0$  to integrate the state equation 2.3 forward from  $t = 0$  to  $t = T$ . The resulting state trajectory  $\mathbf{x}^i$  is stored in the computer memory.
- (3) Use equation 2.6 to compute  $\lambda(T)$  and using  $\mathbf{x}^{(i)}$  computed in (2) and using  $\lambda(T)$  as final condition integrate the costate trajectory 2.5 backwards from  $t = T$  to  $T = 0$ . Evaluate

$$\frac{\partial \mathcal{H}^{(i)}}{\partial \mathbf{u}} = \frac{\partial \mathcal{H}}{\partial \mathbf{u}}(\mathbf{x}^{(i)}(t), \mathbf{u}^{(i)}(t), \lambda^{(i)}(t), t)$$

and store this in memory.

(4) If

$$\left\| \frac{\partial \mathcal{H}^{(i)}}{\partial \mathbf{u}} \right\| \leq \gamma$$

where  $\gamma$  is small positive constant then stop the iteration otherwise go to step (2) using the new controls traversing a small step size  $\tau$  in the direction of the gradient

$$\mathbf{u}^{(i+1)} = \mathbf{u}^{(i)} + \tau \frac{\partial \mathcal{H}^{(i)}}{\partial \mathbf{u}}$$

The maximum principle we described in this section does not directly apply to the case of controlling spin systems to build quantum gates since these systems evolve on Lie groups. However, a generalization of these results and the analogous maximum principle can be described in the context of geometric control theory [Jur97, AS04]. In the case of building quantum gates we look at the control problem dealing with the evolution of the unitary evolution operator given by equation 2.1 . The problem is to drive the unitary evolution operator  $U(t)$  from to a desired target  $U_f$  in time  $T$  minimizing the distance in some norm between the  $\|U(T) - U_f\|$ . For controlling spin systems this is a differential system evolving on a compact Lie group  $\mathcal{G}$ .

$$(2.8) \quad \dot{U}(t) = -i(A + \sum_{k=1}^n v_k(t)B_k)U(t)$$

where  $A$  is the free Hamiltonian (uncontrolled system) and  $\{B_k\}'s$  represent the external control Hamiltonian's and  $v(t)$  are real or complex control amplitudes. The study of controllability of control systems evolving on Lie groups as in the case of spin systems was done in [JS72, AD01b, AD01a] and we have the following theorem.

**THEOREM 2.5.6.** *If the Lie algebra generated by  $A$  and  $\{B_k\}_{k=1}^n$  is equal to  $\mathcal{G}$  then the control system 2.8 is completely controllable.*

In chapter 4 we use a generalization of the maximum principle applied to systems evolving on compact Lie groups to construct quantum gates using the XXZ chain.

## 2.6. Density Matrix Renormalization Group Algorithm

The DMRG method was invented by Steven White in 1992 as an improvement over the real space normalization methods that were not giving accurate results for many models [Whi92]. The original method was very useful in calculating static properties like eigenvalues and correlations functions in strongly correlated one dimensional systems. Recent improvements have resulted in a modification of the DMRG method to study the time evolution of these systems [WF04]. It is now known that the iterative procedure in DMRG, builds what are known as matrix product states [FNW92] and the DMRG method is a variational method within the class of matrix product states [OR95]. More advanced un-

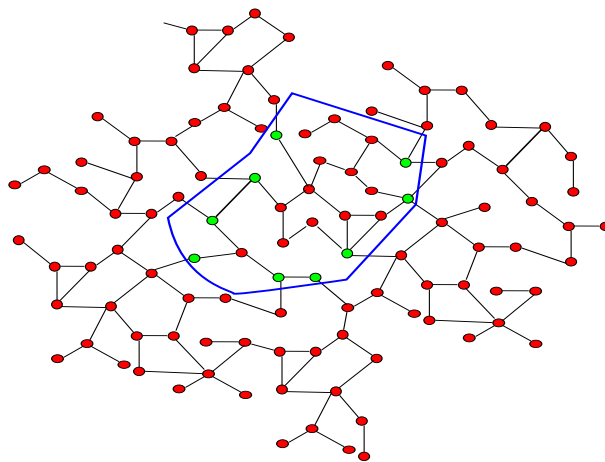


FIGURE 2.6. Area law of entanglement. The area law holds if the entropy of entanglement of a state  $\rho$  between of a distinguished region  $I$  and the rest of the lattice is bounded by a constant times the boundary of the region i.e.  $E(\rho) \leq C|\partial I|$ .

derstanding of the DMRG method had led to connections between the accuracy of the DMRG and the entanglement present in the ground states of the system. Ground states of non-critical one dimensional systems are slightly entangled i.e. the entanglement entropy obeys an area law of entanglement (see figure 2.6) and hence can be efficiently simulated by DMRG. In gapped one dimensional systems the area law was proved in [Has07]. For critical systems one usually finds a logarithmic correction and it is also believed that for local and gapped systems a higher dimensional area law holds [ECP08].

The main issue with accurately describing a quantum system like a spin chain on a computer is that the dimension of the Hilbert space grows exponentially in the length of

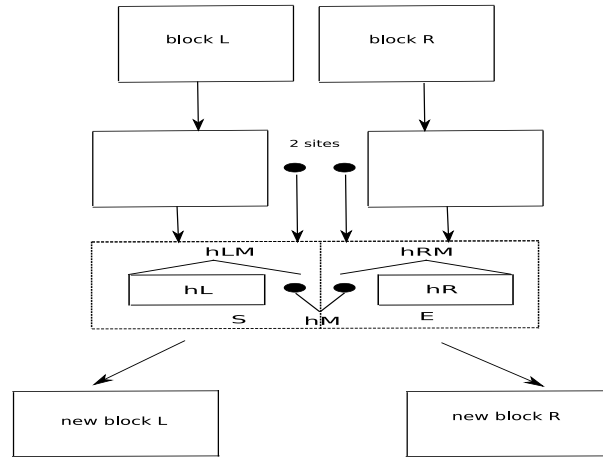


FIGURE 2.7. DMRG truncation procedure

the chain. To counter the growing dimensionality the DMRG procedure iteratively builds the system while truncating the space to preserve only the physically relevant states. The procedure begins with a small number of sites and the descriptions of the interaction of the Hamiltonian on sublattices called blocks. The total Hamiltonian is written in terms of a left block Hamiltonian, two middle sites and right block Hamiltonian and their interactions. The left block and the one middle site to its right combine to form a system block (S) while the right block and the one middle site to its left combine to form a environment block (E). The Hamiltonian of the combined system composed of the system, environment is called the superblock Hamiltonion (see figure 2.7). At each iterative step the chain is grown by adding two sites to the middle and a truncation procedure is carried out with the aim to determine a small set of  $m < \dim(\mathcal{H}_S)$  states which are important to represent a certain state  $|\psi\rangle$  for e.g. ground state (target state) of the superblock. It turns out that these states are the highest weight eigenvectors of the reduced density matrix  $\rho_S := \text{Tr}_E(|\psi\rangle\langle\psi|)$ . The justification for carrying out such a truncation procedure is as follows. Let  $|\psi\rangle$  be represented as

$$|\psi\rangle = \sum_{i,j} \psi_{ij} |i\rangle |j\rangle$$

where  $\{|i\rangle\}$  and  $\{|j\rangle\}$  are orthonormal basis of the system and environment space respectively. We want to find a vector  $|\tilde{\psi}\rangle$  and an orthonormal set  $\{\alpha\}$  of  $\mathcal{H}_S$

$$|\tilde{\psi}\rangle = \sum_{\alpha=1}^m \sum_j \tilde{\psi}_{\alpha j} |\alpha\rangle |j\rangle$$

such that the functional

$$S(\tilde{\psi}) = \|\psi - \tilde{\psi}\|^2$$

is minimized. We interpret the coefficients  $\psi_{ij}$  and  $\tilde{\psi}_{ij}$  as matrices  $\psi = (\psi_{ij})_{ij}$  and  $\tilde{\psi} = (\tilde{\psi}_{ij})_{ij}$  (where rank of  $\tilde{\psi} \leq m$ ) then it is easy to see that the reduced density matrix  $\rho_S$  can be written as  $\rho_S = \psi\psi^\dagger$  and the functional

$$(2.9) \quad S(\tilde{\psi}) = \text{Tr}[(\psi - \tilde{\psi})^\dagger (\psi - \tilde{\psi})]$$

Let  $\psi$  have the Singular Value Decomposition  $\psi = UDV^\dagger$  where  $D = \text{diag}(\lambda_1, \dots, \lambda_n)$  then the singular values  $\{\lambda_1, \dots, \lambda_n\}$  are the square roots of the eigenvalues of  $\rho_S$  since

$$\rho_S = \psi\psi^\dagger = UDV^\dagger V D^\dagger U^\dagger = U D^2 U^\dagger$$

Substituting  $\psi = UDV^\dagger$  into equation 2.9 and using the cyclicity of the trace we get

$$S(\tilde{\psi}) = \text{Tr}[(D - U^\dagger \tilde{\psi} V)^\dagger (D - U^\dagger \tilde{\psi} V)]$$

In this form it is clear that  $S(\tilde{\psi})$  is minimized if we choose we choose  $U^\dagger \tilde{\psi} V$  to be the diagonal matrix  $\tilde{D} = \text{diag}(\lambda_1, \dots, \lambda_m)$ . The  $|\tilde{\psi}\rangle$  that minimizes  $S(\tilde{\psi})$  is given by

$$|\tilde{\psi}\rangle = \sum_{i,j} (U \tilde{D} V^\dagger)_{ij} |i\rangle |j\rangle$$

This can be written as

$$|\tilde{\psi}\rangle = \sum_k \tilde{D}_{kk} \left( \sum_i U_{ik} |i\rangle \right) \otimes \left( \sum_j V_{jk}^* |j\rangle \right)$$

This is the Schmidt decomposition of  $|\psi\rangle$  with only the  $m$  highest weight (largest eigen values)

$$|\tilde{\psi}\rangle = \sum_{\alpha=1}^m \lambda_{\alpha} |v_{\alpha}\rangle |w_{\alpha}\rangle \text{ (Schmidt decomposition)}$$

Thus the relevant states to be kept in the truncation procedure are the  $m$  highest weight eigenvectors of the reduced density matrix  $\rho_S$ . From this, one can also see that the error in the truncation procedure is given by

$$P_m = 1 - \sum_{\alpha=1}^m \lambda_{\alpha}^2$$

If the Schmidt coefficients decay rapidly then the error in the DMRG process will be small. This relates entanglement present in the target state with the efficiency of DMRG. For a Hilbert space of dimension  $m$  we have  $E \leq \log m$ ; alternatively, we need  $m \geq 2^E$  for simulations. Since according to the area law for one dimensional systems  $E$  is bounded by a constant, DMRG yields very precise results for the thermodynamic limit. The failure of DMRG for critical and higher dimensional system is because we need to keep states that grow linearly (critical 1-D systems) and exponentially (dimension  $\geq 2$ ) in the size of the system. The process of increasing the chain by two sites and truncating till the chain is grown to the required length is called the infinite system DMRG procedure. Next a convergence procedure called finite system DMRG is carried out in which left and right Sweep's are carried out in which growth of one block is accompanied by the shrinkage of the other. When one of the blocks reaches a minimum size the growth direction is reversed (see figure 2.8). Usually about 2 or 3 sweeps are required for convergence.

Modifications to the DMRG procedure were made by Vidal to study time evolutions. In [Vid03, Vid04] he considered a quantum spin chain of length  $L$  with a dimension  $d$  at each site and in a state  $|\psi\rangle$ . He showed that the state of a quantum spin chain has  $O(d\chi^2L)$  space requirements where

$$\chi = \max_A \chi_A$$

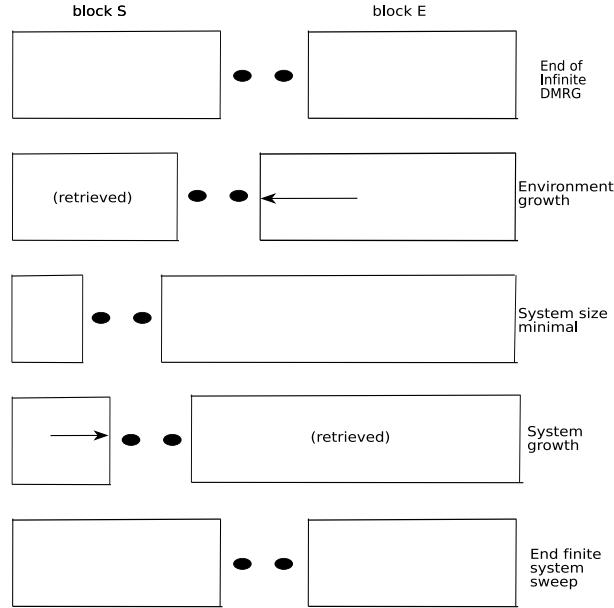


FIGURE 2.8. Finite system DMRG: the convergence procedure

and  $\chi_A$  is the Schmidt rank of the density matrix of  $|\psi\rangle$  and  $A$  is any partition of the chain. Vidal was also able to show that single unitaries and two bit unitaries on this chain could be simulated in  $O(\chi^3)$  operations. This led to the conclusion that if the quantum system was only slightly entangled i.e the Schmidt rank is polynomial in  $L$  then the storage of the state is efficient and single as well as two site unitaries could be efficiently simulated. Note that for a maximally entangled system the Schmidt rank is  $d^{\frac{L}{2}}$  i.e. exponential in  $L$ . Suppose  $H$  was the Hamiltonian of this system, we can write the time evolution in the Trotter decomposition

$$(2.10) \quad e^{-iH\delta} = e^{-\frac{i}{2}h_{-L+1,-L+2}} e^{-\frac{i}{2}h_{-L+2,-L+3}} \dots e^{-\frac{i}{2}h_{L-2,L-1}} e^{-\frac{i}{2}h_{L-1,L}} + O(\delta^3)$$

This leads to efficient simulation of the slightly entangled chain since it involved only 2 site unitaries. White and Feguin were able to reinterpret this in DMRG language [WF04]. The idea is that a two site operator can be applied at sites  $x$  and  $x+1$  to a DMRG state most effectively, by expressing the state in the basis where the left block has length  $x-1$  so the two middle sites that are untruncated are the sites where the operator is applied. Further improvements were made to the time-dependent DMRG methods [DKS<sup>+</sup>05, Kol05] by adaptive time-dependent methods in which the reduced Hilbert space adapts itself (is also time dependent) at each small time step.

We describe the step by step procedure of the DMRG adapted to the XXZ Hamiltonian.

First we carry out the infinite system DMRG procedure as follows:

- (1) Start with the XXZ chain of 4 sites and partition the system into a left block, two middle sites and a right block. The left block with its adjacent middle site form the system block S and the right block along with its adjacent middle site is the environment block E. A static array  $m$  contains the block dimensions. The dimension of the total Hilbert space at each step is  $m(l) \cdot N_{site}^2 \cdot m(L-l-2)$  where  $l$  is the length of the left block,  $m(l)$  is the dimension of the left block,  $N_{site}^2$  is the dimension of the two middle sites,  $L-l-2$  is the length of the right block and  $m(L-l-2)$  is the dimension of the right block.
- (2) Set the total Hamiltonian of this system as the sum of different block operators.

$$H = H^{lt} + H^{lt,mid} + H^{mid} + H^{mid,rt} + H^{rt}$$

$$\begin{aligned}
\text{Left block Hamiltonian} &\equiv H^{lt} = h^{lt} \otimes \mathbb{1} \otimes \mathbb{1} \otimes \underbrace{\mathbb{1} \otimes \dots \otimes \mathbb{1}}_{m(L-l-2) \text{ times}} \\
\text{Left middle interaction Hamiltonian} &\equiv H^{lt,mid} = h^{lt,mid} \otimes \mathbb{1} \otimes \underbrace{\mathbb{1} \otimes \dots \otimes \mathbb{1}}_{m(L-l-1) \text{ times}} \\
\text{Middle sites Hamiltonian} &\equiv H^{mid} = \underbrace{\mathbb{1} \otimes \dots \otimes \mathbb{1}}_{m(l) \text{ times}} \otimes h^{mid} \otimes \underbrace{\mathbb{1} \otimes \dots \otimes \mathbb{1}}_{m(L-l-2) \text{ times}} \\
\text{Middle right interaction Hamiltonian} &\equiv H^{mid,rt} = \underbrace{\mathbb{1} \otimes \dots \otimes \mathbb{1}}_{m(l) \text{ times}} \otimes \mathbb{1} \otimes h^{mid,rt} \\
\text{Right block Hamiltonian} &\equiv H^{rt} = \underbrace{\mathbb{1} \otimes \dots \otimes \mathbb{1}}_{m(l) \text{ times}} \otimes \mathbb{1} \otimes \mathbb{1} \otimes h^{rt}
\end{aligned}$$

The initial values values of ( $L = 4, l = 0$ ) of the blocks are given by taking  $h^{lt} = 0$ ,  $h^{lt,mid} = h_{x,x+1}$ ,  $h^{mid} = h_{x,x+1}$ ,  $h^{mid,rt} = h_{x,x+1}$ ,  $h^{rt} = 0$ , where

$$\begin{aligned}
h_{x,x+1} = J^2(\mathbb{1} \otimes \mathbb{1}) &- S^3 \otimes S^3 - \Delta^{-1}(S^1 \otimes S^1 + S^2 \otimes S^2) \\
&+ J\sqrt{1 - \Delta^{-2}}(S^3 \otimes \mathbb{1} - \mathbb{1} \otimes S^3)
\end{aligned}$$

is the two site XXZ interaction. Since our interest in the low energy states pertaining to a sector, we construct the operator  $S$  corresponding to the total magnetization in the z-direction.

$$S = S^{lt} + S^{mid} + S^{rt}$$

$$\begin{aligned}
\text{Left block magnetization} &\equiv S^{lt} = s^{lt} \otimes \underbrace{\mathbb{I} \otimes \dots \otimes \mathbb{I}}_{m(L-l-2) \text{ times}} \\
\text{Middle sites magnetization} &\equiv S^{mid} = \underbrace{\mathbb{I} \otimes \dots \otimes \mathbb{I}}_{m(l) \text{ times}} \otimes s^{mid} \otimes \underbrace{\mathbb{I} \otimes \dots \otimes \mathbb{I}}_{m(L-l-2) \text{ times}} \\
\text{Right block magnetization} &\equiv S^{rt} = \underbrace{\mathbb{I} \otimes \dots \otimes \mathbb{I}}_{m(l) \text{ times}} \otimes s^{rt}
\end{aligned}$$

Initial values of the magnetization blocks are given by taking  $s^{lt} = S^3$ ,  $s^{mid} = S^3 \otimes \mathbb{I} + \mathbb{I} \otimes S^3$ ,  $s^r = S^3$ .

- (3) Simultaneously diagonalize the the two operators  $H$  and  $S$  and compute the density matrix  $\rho$  consisting of the first(lowest) few eigenvectors of  $H$ . Compute the reduced density matrices  $\rho_S$  and  $\rho_E$  of  $\rho$  corresponding to system and environment respectively. Diagonalize  $\rho_E$  and  $\rho_S$  and retain only the few (say  $m$ ) highest weight eigenvectors of these reduced density matrices and construct the basis transformation matrices  $W^{lt}$  and  $W^{rt}$  consisting of column vectors given by these eigenvectors.
- (4) To carry the iteration forward enlarge the chain by adding two middle sites form new block Hamiltonian's by carrying out the following reduced basis transformations:

$$\begin{aligned}
h^{lt} &\rightarrow (W^{lt})' (h^{lt} \otimes \mathbb{I} + h^{lt,mid}) (W^{lt}) \\
h^{lt,mid} &\rightarrow (W^{lt} \otimes \mathbb{I})' \left( \underbrace{\mathbb{I} \otimes \dots \otimes \mathbb{I}}_{m(l) \text{ times}} \otimes h_{x,x+1} \right) (W^{lt} \otimes \mathbb{I}) \\
h^{mid} &\rightarrow h_{x,x+1} \quad \text{two new sites} \\
h^{mid,rt} &\rightarrow (\mathbb{I} \otimes W^{rt})' (h_{x,x+1} \otimes \underbrace{\mathbb{I} \otimes \dots \otimes \mathbb{I}}_{m(L-l-1) \text{ times}}) (\mathbb{I} \otimes W^{rt}) \\
h^{rt} &\rightarrow (W^{rt})' (\mathbb{I} \otimes h^{rt,mid} + h^{rt}) (W^{rt})
\end{aligned}$$

$$\begin{aligned}
s^{lt} &\rightarrow (W^{lt})' \left( s^{lt} \otimes \mathbb{1} + \underbrace{\mathbb{1} \otimes \cdots \otimes \mathbb{1}}_{m(l) \text{ times}} \otimes S^3 \right) (W^{lt}) \\
s^{rt} &\rightarrow (W^{rt})' \left( \mathbb{1} \otimes s^{rt} + S^3 \otimes \underbrace{\mathbb{1} \otimes \cdots \otimes \mathbb{1}}_{m(L-l-1) \text{ times}} \right) (W^{rt}) \\
L &\rightarrow L + 2 \\
l &\rightarrow l + 1
\end{aligned}$$

- (5) If  $L$  is equal to the final chain length desired then end infinite system DMRG otherwise we go to step (2).

The finite system DMRG and the time-dependent procedures are carried out as usual. For further reading on DMRG, an excellent review is given in [Sch05, Sch07].

## CHAPTER 3

## Isolated Eigenvalues

## 3.1. Introduction

In this chapter<sup>1</sup> we are investigating the existence of isolated excited states at the domain walls, called kinks, in one-dimensional magnetic systems. It turns out that if the spins are of magnitude  $3/2$  or more and their interactions have a suitable anisotropy, such as in the ferromagnetic XXZ Heisenberg model, isolated excited states are possible. For the spin  $1/2$  and spin  $1$  chains, however, the ground states are simply separated by a gap to the rest of the spectrum and there are no isolated excited states below the continuum.

Our main result is a mathematical demonstration that such states indeed exist for sufficiently large anisotropy.

Concretely, we study the one-dimensional spin  $J$  ferromagnetic XXZ model with the following boundary terms. The Hamiltonian is

$$H_L^k(\Delta^{-1}) = \sum_{\alpha=-L}^{L-1} \left[ (J^2 - S_\alpha^3 S_{\alpha+1}^3) - \Delta^{-1} (S_\alpha^1 S_{\alpha+1}^1 + S_\alpha^2 S_{\alpha+1}^2) \right] + J \sqrt{1 - \Delta^{-2}} (S_{-L}^3 - S_L^3)$$

where  $S_\alpha^1, S_\alpha^2$  and  $S_\alpha^3$  are the spin  $J$  matrices acting on the site  $\alpha$ . Apart from the magnitude of the spins,  $J$ , the main parameter of the model is the anisotropy  $\Delta > 1$  and we will refer to the limit  $\Delta \rightarrow \infty$  as the *Ising limit*. In the case of  $J = 1/2$  these boundary conditions were first introduced in [PS90]. They lead to ground states with a domain wall between down spins on the left portion of the chain and up spins on the right. The domain wall is exponentially localized. The third component of the magnetization,  $M$ , is conserved, and there is exactly one ground state for each value of  $M$ . Different values of  $M$  correspond to different positions of the domain walls, which in one dimension are sometimes referred to as kinks. In [ASW95] and [GW96] the ground states for this type boundary conditions were further analyzed and generalized to higher spin,  $J$ . A careful analysis of the Ising limit (see Section 3.4), reveals that something special happens for  $J = 3/2$  and larger: one

<sup>1</sup>The text of this chapter is essentially a reprint of the paper *Journal of Stat. Mech.* **P01016** 2008

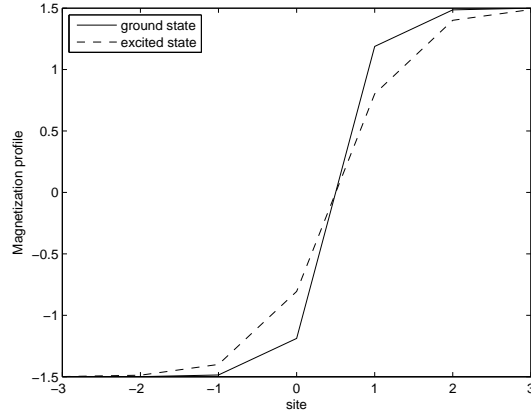


FIGURE 3.1. The ground state and first excited state of the XXZ chain of length 7 with  $J = \frac{3}{2}$ ,  $\Delta = 2.5$  in the sector  $M = -3/2$ .

or more low-lying excitations turn out to be also domain wall states of finite degeneracy, and therefore one should expect them to persist under perturbations. In particular, in this paper we show these states exist as isolated eigenvalues in the XXZ chain with sufficiently strong anisotropy. This is illustrated in Figure 3.1. Moreover, as a consequence of the strong localization of these states near the position of the ground state kink, these eigenvalues only weakly depend on the distance of the domain wall to the edges of the chain and persist in the thermodynamic limit. In the thermodynamic limit the perturbation of the entire chain corresponds to an unbounded operator. Standard finite-order perturbation theory is therefore inadequate. The mathematical theory of how to handle this situation is described in Section 3.5.2. We now describe the structure of the ground states a bit more explicitly.

Our main result is a proof that for all sufficiently large  $\Delta$  the first few excitations of the XXZ model are isolated eigenvalues. This is true for all  $J \geq \frac{3}{2}$  and for spin 1 with  $M$  even, which is illustrated in Figure 3.1 for the spin  $3/2$  and spin 2 chains. See Section 3.3 for the precise statements. It turns out that in the Ising limit the eigenvalues less than  $2J$  are all of multiplicity at most 2 in each sector. Moreover, the first excited states are simple except in the case when  $J > 1$  is an integer and  $M = 0 \pmod{2J}$ . In this case, they are doubly degenerate. This is discussed in Section 3.4. In Section 3.5, we write the XXZ Hamiltonian as an explicit perturbation of the Ising limit. Theorem 3.5.3 verifies that the perturbation is relatively bounded with respect to the Ising limit, and we finish this section by demonstrating that our estimates suffice to guarantee analytic continuation of

the limiting eigenvalues. It is clear that the same method of proof can be applied to other Hamiltonians.

While the question of low-lying excitations is generally interesting, it may be particularly important in the context of quantum computation. For quantum computers to become a reality we need to find or build physical systems that faithfully implement the quantum gates used in the algorithms of quantum computation [Sho97]. The basic requirement is that the experimenter has access to two states of a quantum system that can be effectively decoupled from environmental noise for a sufficiently long time, and that transitions between these two states can be controlled to simulate a number of elementary quantum gates (unitary transformations). Systems that have been investigated intensively are single photon systems, cavity QED, nuclear spins (using NMR in suitable molecules), atomic levels in ion traps, and Josephson rings [NC00, MOL<sup>+</sup>99, CVZ<sup>+</sup>98]. We believe that if one could build one-dimensional spin  $J$  systems with  $J \geq 3/2$ , which interact through an anisotropic interaction such as in the XXZ model, this would be a good starting point to encode qubits and unitary gates. The natural candidates for control parameters in such systems would be the components of a localized magnetic field. From the experimental point of view this is certainly a challenging problem. This work is a first step toward a mathematical model to study the optimal control of these systems such as has already been carried out for nuclear magnetic resonance (NMR) [KBG01, MK05] and superconducting Josephson qubits [Gal07].

### 3.2. Set-up

We study the spin  $J$  ferromagnetic XXZ model on the one-dimensional lattice  $\mathbb{Z}$ . The local Hilbert space for a single site  $\alpha$  is  $\mathcal{H}_\alpha = \mathbb{C}^{2J+1}$  with  $J \in \frac{1}{2}\mathbb{N} = \{0, \frac{1}{2}, 1, \frac{3}{2}, 2, \dots\}$ . We consider the Hilbert space for a finite chain on the sites  $[-L, L] = \{-L, -L+1, \dots, +L\}$ . This is  $\mathcal{H}_{[-L, L]} = \bigotimes_{\alpha=-L}^L \mathcal{H}_\alpha$ . The Hamiltonian of the spin- $J$  XXZ model is

$$(3.1) \quad H_L(\Delta^{-1}) = \sum_{\alpha=-L}^{L-1} h_{\alpha, \alpha+1}(\Delta^{-1}),$$

$$h_{\alpha, \alpha+1}(\Delta^{-1}) = J^2 - S_\alpha^3 S_{\alpha+1}^3 - \Delta^{-1} (S_\alpha^1 S_{\alpha+1}^1 + S_\alpha^2 S_{\alpha+1}^2),$$

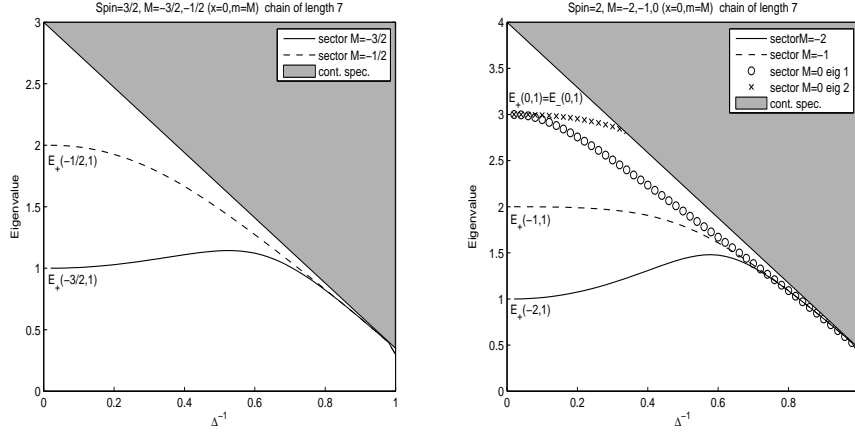


FIGURE 3.2. The low-lying spectrum of the XXZ model for  $J = \frac{3}{2}$  and  $J = 2$  for various sectors. Note the two-fold degeneracy for spin 2 in the sector  $M = 0$  corresponding to  $E_+(0, 1) = E_-(0, 1)$ . The shaded region contains those eigenvalues which converge to continuous spectrum in the thermodynamic limit. We note that, for  $\Delta = 1$ , the gap vanishes in the thermodynamics limit.

where  $S_\alpha^1, S_\alpha^2$  and  $S_\alpha^3$  are the spin- $J$  matrices acting on the site  $\alpha$ , tensored with the identity operator acting on the other sites. The main parameter of the model is the anisotropy  $\Delta > 1$  and we get the Ising limit as  $\Delta \rightarrow \infty$ . It is mathematically more convenient to work with the parameter  $\Delta^{-1}$ , which we then assume is in the interval  $[0, 1]$ . As we said,  $\Delta^{-1} = 0$  is the Ising limit, and  $\Delta^{-1} = 1$  is the isotropic XXX Heisenberg model. It was shown [PS90, ASW95, GW96, KN98] that additional ground states emerge when we add particular boundary terms. Examples of this are the kink and antikink Hamiltonians

$$(3.2) \quad H_L^k(\Delta^{-1}) = H_L(\Delta^{-1}) + J\sqrt{1 - \Delta^{-2}}(S_{-L}^3 - S_L^3)$$

$$(3.3) \quad H_L^{\text{ak}}(\Delta^{-1}) = H_L(\Delta^{-1}) - J\sqrt{1 - \Delta^{-2}}(S_{-L}^3 - S_L^3)$$

It is easy to see that the *kink* and *anti-kink* Hamiltonians are unitarily equivalent. We will be mainly interested in the *kink* Hamiltonian with  $L \geq 2$ . Note that, by a telescoping sum, we can absorb the boundary fields into the local interactions:

$$(3.4) \quad H_L^k(\Delta^{-1}) = \sum_{\alpha=-L}^{L-1} h_{\alpha, \alpha+1}^k(\Delta^{-1}),$$

$$h_{\alpha, \alpha+1}^k(\Delta^{-1}) = J^2 - S_\alpha^3 S_{\alpha+1}^3 - \Delta^{-1}(S_\alpha^1 S_{\alpha+1}^1 + S_\alpha^2 S_{\alpha+1}^2) + J\sqrt{1 - \Delta^{-2}}(S_\alpha^3 - S_{\alpha+1}^3)$$

The Ising kink Hamiltonian is the result of taking  $\Delta \rightarrow \infty$ , equivalently setting  $\Delta^{-1} = 0$ , namely it is

$$(3.5) \quad \begin{aligned} H_L^k(0) &= \sum_{\alpha=-L}^{L-1} h_{\alpha,\alpha+1}^k(0), \\ h_{\alpha,\alpha+1}^k(0) &= (J^2 - S_\alpha^3 S_{\alpha+1}^3) + J(S_\alpha^3 - S_{\alpha+1}^3) \\ &= (J + S_\alpha^3)(J - S_{\alpha+1}^3). \end{aligned}$$

Each of the Hamiltonians introduced above commutes with the total magnetization

$$S_{\text{tot}}^3 = \sum_{\alpha=-L}^L S_\alpha^3.$$

As indicated in the introduction to this chapter, for each  $M \in \{-J(2L+1), \dots, J(2L+1)\}$ , the corresponding sector is defined to be the eigenspace of  $S_{\text{tot}}^3$  with eigenvalue  $M$ ; clearly, these are invariant subspaces for all the Hamiltonians introduced above.

The Ising basis is a natural orthonormal basis for  $\mathcal{H}_{[-L,L]}$ . At each site we have an orthonormal basis of the Hilbert space  $\mathcal{H}_\alpha$  given by the eigenvectors of  $S_\alpha^3$  and labeled according to their eigenvalues. We will denote this by  $S_\alpha^3 |m\rangle_\alpha = m |m\rangle_\alpha$  for  $m \in [-J, J]$ , and  $\alpha \in [-L, L]$ . Here, and throughout the remainder of the paper, we will use the notation  $[-J, J]$  for the set  $\{-J, -J+1, \dots, J\}$  as we have done with  $[-L, L]$ . Finally, there is an orthonormal basis of the entire Hilbert space consisting of simple tensor product vectors:  $\bigotimes_{\alpha=-L}^L |m_\alpha\rangle_\alpha$ .

Also recall that the raising and lowering operators are defined such that

$$\begin{aligned} S_\alpha^+ |m\rangle_\alpha &= \begin{cases} \sqrt{J(J+1) - m(m+1)} |m+1\rangle_\alpha & \text{if } -J \leq m \leq J-1, \\ 0 & \text{if } m = J; \end{cases} \\ S_\alpha^- |m\rangle_\alpha &= \begin{cases} \sqrt{J(J+1) - m(m-1)} |m-1\rangle_\alpha & \text{if } -J+1 \leq m \leq J, \\ 0 & \text{if } m = -J. \end{cases} \end{aligned}$$

A short calculation shows that  $S_\alpha^1$  and  $S_\alpha^2$  are given by  $S_\alpha^1 = (S_\alpha^+ + S_\alpha^-)/2$  and  $S_\alpha^2 = (S_\alpha^+ - S_\alpha^-)/2i$ , and

$$S_\alpha^1 S_{\alpha+1}^1 + S_\alpha^2 S_{\alpha+1}^2 = \frac{1}{2} (S_\alpha^+ S_{\alpha+1}^- + S_\alpha^- S_{\alpha+1}^+).$$

### 3.3. Main theorem

Many of the results in this chapter concern the *kink* Hamiltonian given by (3.4). We will study it as a perturbation of the Ising Hamiltonian (3.5) in the regime  $0 < \Delta^{-1} \ll 1$ . We denote an Ising configuration as  $\vec{m} = (m_\alpha)_{\alpha=-L}^L$ , where  $m_\alpha \in [-J, J]$  for each  $\alpha$ , and the corresponding basis vector as

$$|\vec{m}\rangle = \bigotimes_{\alpha=-L}^L |m_\alpha\rangle_\alpha.$$

Observe that the Ising *kink* Hamiltonian is diagonal with respect to this basis,

$$(3.6) \quad \begin{aligned} H_L^k(0) |\vec{m}\rangle &= E^k(\vec{m}) |\vec{m}\rangle, \quad \text{where} \\ E^k(\vec{m}) &= \sum_{\alpha=-L}^{L-1} e^k(m_\alpha, m_{\alpha+1}) \quad \text{and} \\ e^k(m_\alpha, m_{\alpha+1}) &= (J + m_\alpha)(J - m_{\alpha+1}). \end{aligned}$$

Since each of the  $e^k(m_\alpha, m_{\alpha+1})$  are non-negative, it is easy to see that the ground states of  $H_L^k(0)$  are all of the form

$$(3.7) \quad \Psi_0(x, m; L) = |\vec{m}\rangle, \quad \text{where} \quad m_\alpha = \begin{cases} -J & \text{for } -L \leq \alpha \leq x-1 \\ m & \text{for } \alpha = x \\ J & \text{for } x+1 \leq \alpha \leq L, \end{cases}$$

with some  $x \in [-L, L]$  and  $m \in [-J, J]$ . Note that the total magnetization corresponding to  $\Psi_0(x, m; L)$  is  $M = -2Jx + m$ . As we will verify in Proposition 3.4.1, it is easy to check that these ground states are unique per sector. We do point out that there is a slight ambiguity in the above labeling scheme, however, since  $\Psi_0(x-1, -J; L)$  and  $\Psi_0(x, J; L)$  coincide. Let us consider the following elementary result.

**THEOREM 3.3.1.** *For  $J \in \frac{1}{2}\mathbb{N}$ ,  $L \geq 2$  and  $M \in \{-J(2L+1), \dots, J(2L+1)\}$ , the eigenspace of  $H_L^k(0)$  corresponding to energy  $E = 2J$  has dimension at least equal to  $2L+1$ .*

Because of this theorem, we see that, in the  $L \rightarrow \infty$  limit, the energy  $E = 2J$  is essential spectrum; an eigenvalue with infinite multiplicity. As our interest is in perturbation theory,

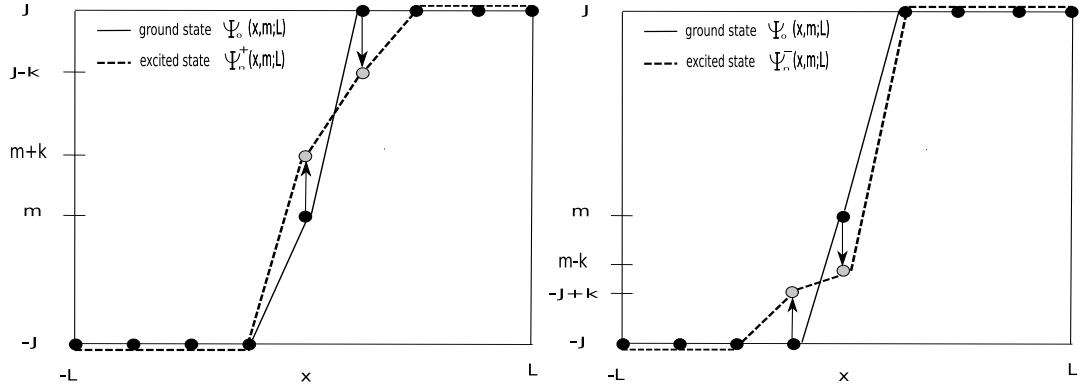


FIGURE 3.3. The two kinds of low lying Ising excitations. The left picture belongs to the set  $K_+(m)$  and the right to the set  $K_-(m)$ .

it is natural for us to restrict our attention to energies strictly between 0 and  $2J$ . We will call the corresponding eigenvectors “low energy excitations”.

We will now describe all the low energy excitations for the Ising kink Hamiltonian. In order to do so, it is convenient to introduce a family of eigenvectors which contains all possible low energy excitations.

Let  $x$  be any site away from the boundary, i.e. take  $x \in [-L + 1, L - 1]$ , and choose  $m \in [-J, J]$ . These choices specify a sector  $M = -2Jx + m$  and a groundstate  $\Psi_0(x, m; L)$ . If  $m < J$ , we define the following vectors: For  $1 \leq n \leq J - m$  set

$$(3.8) \quad \Psi_n^+(x, m; L) = |\vec{m}\rangle, \quad \text{where } m_\alpha = \begin{cases} -J & \text{if } \alpha \leq x - 1, \\ m + n & \text{if } \alpha = x, \\ J - n & \text{if } \alpha = x + 1, \\ J & \text{if } \alpha \geq x + 2. \end{cases}$$

If  $-J < m$ , we define the following vectors: For  $1 \leq n \leq J + m$  set

$$(3.9) \quad \Psi_n^-(x, m; L) = |\vec{m}\rangle, \quad \text{where } m_\alpha = \begin{cases} -J & \text{if } \alpha \leq x - 2, \\ -J + n & \text{if } \alpha = x - 1, \\ m - n & \text{if } \alpha = x, \\ J & \text{if } \alpha \geq x + 1. \end{cases}$$

We call these two sequences of Ising basis vectors the “localized kink excitations”. Clearly, these vectors  $\{\Psi_n^\pm(x, m; L)\}$  have the same total magnetization  $M$  and moreover,

$$(3.10) \quad H_L^k(0) \Psi_n^\pm(x, m; L) = E_\pm(m, n) \Psi_n^\pm(x, m; L), \text{ with } E_\pm(m, n) = n^2 + (J \pm m)n,$$

where  $E_\pm(m, n)$  has been calculated using (3.6); note that in each case there is only one non-zero term. In Figure 3.3 we have shown two ground states, in the left and right graphs, as well as two low excitations. These are the schematic diagrams for  $\Psi_0(x, m)$ , in solid in both pictures, and  $\Psi_k^+(x, m)$  and  $\Psi_k^-(x, m)$ , in a dashed line, in the left and right, respectively

We now define two sets of labels:

$$(3.11) \quad K_\pm(m) = \{n : n \in \mathbb{N}, 1 \leq n \leq J \mp m, E_\pm(m, n) < 2J\}.$$

Depending on  $m$  and  $J$ , neither, one, or both of these sets may be empty. We have the following theorem.

**THEOREM 3.3.2.** (1) *The low energy excitations of  $H_L^k(0)$  form a subset of the localized kink excitations introduced in (3.8) and (3.9) above.*

(2) *For  $M$  of the form  $M = -2Jx + m$  with some  $x \in [-L + 1, L - 1]$  and  $m \in [-J, J]$ , the set of low energy excitations equals*

$$\{\Psi_n^+(x, m; L) : n \in K_+(m)\} \cup \{\Psi_n^-(x, m; L) : n \in K_-(m)\}.$$

*This is a nonempty set except in the following two cases:  $J = \frac{1}{2}$ , or  $J = 1$ , and  $m = 0$ .*

(3) *The low energy excitations of  $H_L^k(0)$  are at most two-fold degenerate. The first excitation is simple, except for the case that  $J$  is an integer  $J > 1$ , and  $M = 0 \pmod{2J}$ .*

**REMARK 3.3.3.** *The two-fold degeneracy of the first excited state, guaranteed by part (3) of the theorem, occurs due to the spin flip and reflection symmetry. All other degeneracies with energy  $< 2J$  occur as follows. Suppose  $2J = ab$  for integers  $2 \leq a \leq b$ . In this case, let  $m = J - 2 + a - b$ . Then  $\Psi_1^+(x, m; L)$  is degenerate with  $\Psi_{a-1}^-(x, m; L)$ , both with energy  $2J - 1 + a - b$ . Similarly,  $\Psi_1^-(x, -m; L)$  is degenerate with  $\Psi_{a-1}^+(x, -m; L)$  for the same energy.*

Next we consider the perturbed Hamiltonian  $H_L^k(\Delta^{-1})$ . As is discussed in Section 3.5.2, each low-lying eigenvalue  $E_{\pm}(m, n)$ , associated to some  $n \in K_{\pm}(m)$ , is isolated from the rest of the spectrum by an isolation distance  $d_{\pm}(m, n) \geq 1$ , independent of  $L$ , which is defined by

$$d_{\pm}(m, n) = \inf_{E \in \sigma(H_L^k(0)) \setminus \{E_{\pm}(m, n)\}} |E - E_{\pm}(m, n)|.$$

**THEOREM 3.3.4.** *Let  $L \geq 2$ , and fix  $J \geq \frac{3}{2}$ . For any  $n \in K_{\pm}(m)$ , consider the interval  $I = [E_{\pm}(m, n) - d_{\pm}(m, n)/2, E_{\pm}(m, n) + d_{\pm}(m, n)/2]$  about the low lying energy  $E_{\pm}(m, n)$ . The spectral projection of  $H_L^k(\Delta^{-1})$  onto  $I$  is analytic for large enough values of  $\Delta$ . In particular, the dimension of the spectral projection onto  $I$  is constant for this range of  $\Delta$ .*

**REMARK 3.3.5.** *Our estimates yield a lower bound on  $\Delta$  as is provided by (3.52). A slightly worse bound demonstrates that taking  $\Delta > 18J^{5/2}$  suffices, but we do not expect either estimate to be sharp.*

The above theorem confirms the structure of the spectrum shown in Figure 3.1. Moreover, since our numerical calculations indicate that some of the eigenvalues enter the continuous spectrum, we do not expect this type of perturbation theory to work for the entire range of  $\Delta^{-1} \in [0, 1]$ .

### 3.4. Proof of Theorems 3.3.1 and 3.3.2 (Excitations of the Ising Model)

In this section, we will focus on the Ising kink Hamiltonian  $H_L^k(0)$ , as introduced in (3.5), for a fixed  $J \in \frac{1}{2}\mathbb{N}$ . The ground states can be characterized as follows:

**PROPOSITION 3.4.1.** *The ground states of the Ising kink Hamiltonian are all of the form*

$$(3.12) \quad \Psi_0(x, m; L) = |\vec{m}\rangle, \quad \text{where} \quad m_{\alpha} = \begin{cases} -J & \text{for } \alpha = -L, \dots, x-1, \\ m & \text{for } \alpha = x, \\ +J & \text{for } \alpha = x+1, \dots, L; \end{cases}$$

for  $x \in [-L, \dots, L]$  and  $m \in [-J, J]$ . Moreover, there is exactly one ground state in each sector; the total magnetization eigenvalue for  $\Psi_0(x, m; L)$  is  $M = 2Jx + m$ .

This proposition was already used, implicitly, in setting up Theorem 3.3.2. Here we prove it.

**Proof:** Given any Ising configuration  $\vec{m} = (m_\alpha)_{\alpha=-L}^L$ , equation (3.6) demonstrates that the energy associated to  $|\vec{m}\rangle$ ,  $E^k(\vec{m})$ , is the sum of  $2L$  non-negative terms. Therefore, the only way to have  $E^k(\vec{m}) = 0$  is if all of the summands are 0. This is the case only if either  $m_\alpha = -J$  or  $m_{\alpha+1} = +J$  for all  $\alpha$ . Clearly, this is satisfied for the Ising configurations with  $m_\alpha = -J$  for all  $\alpha < x$ ,  $m_\alpha = +J$  for all  $\alpha > x$ , and  $m_x$  equal to any number in  $[-J, J]$ . It is equally easy to see that these are all of the ground state configurations: if  $\vec{m}$  is a groundstate configuration and for some  $x$  we have  $m_x \neq -J$ , then  $m_{x+1} = J$ , which, by induction, means that  $m_\alpha = +J$  for all  $\alpha > x$ . Similar reasoning yields that  $m_\alpha = -J$  for all  $\alpha < x$ .

To show that the ground states are unique in each sector, consider the equation  $M - m = -2Jx$ , subject to the constraints:  $M \in \{-J(2L + 1), \dots, J(2L + 1)\}$ ,  $m \in [-J, J]$ , and  $x \in [-L, L]$ . If  $M - J \not\equiv 0 \pmod{2J}$ , then there is a unique pair  $(x, m)$  which satisfies this equation. If  $M - J \equiv 0 \pmod{2J}$ , then there are two possible solutions  $(x, J)$  and  $(x - 1, -J)$  for some  $x$ . But then, it is trivial to see that  $\Psi_0(x, J; L)$  and  $\Psi_0(x - 1, -J; L)$  coincide. ■

Thus in any sector  $M$ , there is a unique ground state eigenvector  $\Psi_0(x, m; L)$  for some choice of  $(x, m)$  with  $M = -2Jx + m$ . We next observe that there are many eigenvectors with eigenvalue  $2J$ ; recall this was the statement of Theorem 3.3.1.

**Proof of Theorem 3.3.1:** First consider the case that  $M - J$  is not divisible by  $2J$ . Then the unique groundstate eigenvector is  $\Psi_0(x, m; L)$  for some  $x \in [-L, L]$  and  $-J < m < J$ . If  $x > -L$ , then for each  $y \in [-L, x - 2]$  consider the Ising configuration  $\vec{m}$  with components

$$m_\alpha = \begin{cases} -J & \text{if } \alpha \leq x - 1 \text{ and } \alpha \neq y; \\ -J + 1 & \text{if } \alpha = y; \\ m - 1 & \text{if } \alpha = x; \\ J & \text{if } \alpha \geq x + 1. \end{cases}$$

The total magnetization for the vector  $|\vec{m}\rangle$  is still  $M$ . Using the formula (3.6) again, it is easy to check that  $e^k(m_y, m_{y+1}) = 2J$ ,  $e^k(m_\alpha, m_{\alpha+1}) = 0$  for all  $\alpha \neq y$ , and therefore,  $E^k(\vec{m}) = 2J$ . This constitutes  $x - 1 + L$  possible values of  $y$ ; producing at least this many distinct eigenvectors with energy  $2J$ . Similarly, if  $x < L$  then there are  $L - x - 1$  Ising

configurations of the form  $\vec{m}$  with components

$$m_\alpha = \begin{cases} -J & \text{if } \alpha \leq x-1; \\ m+1 & \text{if } \alpha = x; \\ J-1 & \text{if } \alpha = y; \\ J & \text{if } \alpha \geq x+1 \text{ and } \alpha \neq y; \end{cases}$$

corresponding to some  $y \in [x+2, L]$ . In total, this gives  $2L-2$  orthonormal eigenvectors corresponding to eigenvalue  $2J$ , yielding a lower bound on the dimension of the eigenspace. If  $x = -L$  or  $L$ , then the dimension is increased by at least 1. In the special case where  $M-J$  is divisible by  $2J$ , the eigenvector can be written in two ways as  $\Psi_0(x, J; L)$  or  $\Psi_0(x-1, -J; L)$ . When constructing excitations for  $y$  to the left of the kink, use the first formula above relative to  $\Psi_0(x, J; L)$ . When constructing excitations for  $y$  to the right of the kink, use the second formula above relative to  $\Psi_0(x-1, -J; L)$ . Once again, this results in  $2L-1$  orthonormal eigenvectors corresponding to eigenvalue  $2J$ .  $\blacksquare$

We now claim that any Ising configuration which is neither a ground state nor a localized kink excitation corresponds to an energy that is at least  $2J$ . This is the content of the following lemma.

LEMMA 3.4.2. *Consider an Ising configuration  $\vec{m} = (m_\alpha)_{\alpha=-L}^L$ .*

- (1) *If there is any  $x \in [-L, L-1]$  such that  $m_x > m_{x+1}$ , then  $E^k(\vec{m}) \geq 2J$ .*
- (2) *If there is any  $x \in [-L+1, \dots, L-1]$  such that  $m_{x-1} > -J$  and  $m_{x+1} < J$ , then  $E^k(\vec{m}) \geq 2J$ .*

**Proof:** (1) It is clear from (3.6) that we need only prove

$$(3.13) \quad J^2 - m_x m_{x+1} + J(m_x - m_{x+1}) = e^k(m_x, m_{x+1}) \geq 2J.$$

Since  $m_x > m_{x+1}$ , we have that  $J(m_x - m_{x+1}) \geq J$ . We need only verify that  $J^2 - m_x m_{x+1} \geq J$  to establish the claim. The product of two integers  $m_x, m_{x+1} \in [-J, J]$  is at most equal to  $J^2$ . But this is only attained by  $m_x = m_{x+1} = \pm J$ . Since  $m_x > m_{x+1}$ , we can neither have  $m_{x+1} = J$  nor  $m_x = -J$ . The next largest possible value of  $m_x m_{x+1}$  is  $J(J-1)$ , and we have verified the claim.

(2) Again, because all terms are nonnegative, it suffices to show that

$$e^k(m_{x-1}, m_x) + e^k(m_x, m_{x+1}) \geq 2J.$$

Using the formula for  $e^k(\cdot, \cdot)$  and simplifying gives

$$e^k(m_{x-1}, m_x) + e^k(m_x, m_{x+1}) = 2J^2 + J(m_{x-1} - m_{x+1}) - m_x(m_{x-1} + m_{x+1}).$$

Since  $|m_x| \leq J$ , we have

$$\begin{aligned} e^k(m_{x-1}, m_x) + e^k(m_x, m_{x+1}) &\geq 2J^2 + J(m_{x-1} - m_{x+1}) - J|m_{x-1} + m_{x+1}| \\ &= J(2J + m_{x-1} - m_{x+1} - |m_{x-1} + m_{x+1}|). \end{aligned}$$

Therefore,

$$e^k(m_{x-1}, m_x) + e^k(m_x, m_{x+1}) \geq \begin{cases} 2J(J - m_{x+1}) & \text{if } m_{x-1} + m_{x+1} \geq 0; \\ 2J(J + m_{x-1}) & \text{if } m_{x-1} + m_{x+1} \leq 0. \end{cases}$$

Since  $J - m_{x+1} \geq 1$  and  $J + m_{x-1} \geq 1$ , in either case we have proven the claim.  $\blacksquare$

Now we can finish the proof of the first main result, Theorem 3.3.2.

**Proof of Theorem 3.3.2:** Part (1) of the theorem is a direct consequence of Lemma 3.4.2 because the only Ising configurations that do not satisfy condition (1) or (2) of that lemma are the ground state configurations and the localized kink excitations.

To prove part (2), let  $M = -2Jx + m$  for some  $x \in [-L + 1, L - 1]$  and  $m \in [-J, J]$ .

We first consider the case that  $J \geq 3/2$ .

If  $J$  is sufficiently large and  $|m| \leq J - 2$ , then  $n = 1 \in K_{\pm}(m)$  as

$$E_{\pm}(m, 1) = 1^2 + (J \pm m)1 \leq 1 + J + |m| < 2J.$$

So, in this case, both  $K_+(m)$  and  $K_-(m)$  are nonempty.

Similarly, if  $|m| = J - 1$ , then either

$$E_+(-J + 1, 1) = 1^2 + (J + (-J + 1))1 = 2,$$

or

$$E_-(J-1, 1) = 1^2 + (J - (J-1))1 = 2.$$

Hence,  $1 \in K_+(m) \cup K_-(m)$  if  $|m| = J-1$  and  $J \geq 3/2$ .

Lastly, if  $|m| = J$ , then either

$$E_+(-J, 1) = 1^2 + (J + (-J))1 = 1,$$

or

$$E_-(J, 1) = 1^2 + (J - J)1 = 1.$$

Hence,  $1 \in K_+(m) \cup K_-(m)$  if  $|m| = J-1$  and  $J \geq 1$ .

We have proved (2) in the case that  $J \geq 3/2$ . Actually, the last observation above also verifies (2) in the case that  $J = 1$  and  $m = \pm 1$ .

Finally, if  $J = 1$  and  $m = 0$ , then  $E_{\pm}(0, 1) = 1^2 + (1 \pm 0) = 2$  and if  $J = 1/2$ , then  $E_{\pm}(\mp 1/2, 1) = 1^2 + (1/2 - 1/2) = 1$ . In both these cases, the set of kink excitations is empty.

We now prove the first part of (3). First, observe that for any  $m \in [-J, J]$ ,  $J \pm m \geq 0$  and therefore with  $m$  fixed, both  $E_{\pm}(m, n)$  are increasing functions of  $n$  for  $n \geq 0$ . Therefore the only degeneracies that can occur for a particular energy  $E$  is if  $E_+(m, n_1) = E$  and  $E_-(m, n_2) = E$  for some integers  $n_1$  and  $n_2$ . This is obviously at most a two-fold degeneracy.

In order to prove the second part of (3), we will simply prove Remark 3.3.3. Without loss of generality, suppose  $m \geq 0$ . Then  $E_+(m, 2) = 4 + 2J + 2m > 2J$ . So the only possibility for  $E_+(m, n)$  to be less than  $2J$  is if  $n = 1$ , which gives the energy  $J + m + 1$  and an auxiliary condition, namely  $J - m \geq 2$ . A degeneracy happens only if there is a  $p \geq 1$  such that  $E_-(m, p) = E_+(m, 1)$ . This means

$$p^2 + (J - m)p = J + m + 1 \quad \iff \quad (p + 1)(p + J - m - 1) = 2J.$$

Setting  $a = p + 1$  and  $b = p + J - m - 1$  (which satisfies  $b \geq a$  because  $J - m \geq 2$ ) we have exactly the result claimed. Note that the second part of (3) refers to the first excitation. For  $m \geq 0$ , the lowest excitation is  $E_-(m, 1)$ . This means  $p = 1$ , which implies  $m = 0$  and therefore  $2J$  is even with  $J \geq 2$  (because  $J - m \geq 2$ ).

■

### 3.5. Proof of the main theorem

The goal of this section is to prove Theorem 3.3.4. We will do so by analyzing the kink Hamiltonian  $H_L^k(\Delta^{-1})$  as a perturbation of the Ising limit  $H_L^k(0)$ . Within the first subsection below, specifically in Theorem 3.5.3, we prove that the operators which arise in our expansion of  $H_L^k(\Delta^{-1})$  are relatively bounded with respect to  $H_L^k(0)$ . In the next subsection, we discuss how the explicit bounds on  $\Delta$ , those claimed in Theorem 3.3.4, follow from relative boundedness and basic perturbation theory.

**3.5.1. Relative Boundedness.** In this subsection, we will analyze the kink Hamiltonian introduced in (3.4). Recall that this Hamiltonian is written as

$$(3.14) \quad H_L^k(\Delta^{-1}) = \sum_{\alpha=-L}^{L-1} h_{\alpha,\alpha+1}^k(\Delta^{-1}),$$

$$h_{\alpha,\alpha+1}^k(\Delta^{-1}) = J^2 - S_\alpha^3 S_{\alpha+1}^3 - \Delta^{-1}(S_\alpha^1 S_{\alpha+1}^1 + S_\alpha^2 S_{\alpha+1}^2) + J\sqrt{1 - \Delta^{-2}}(S_\alpha^3 - S_{\alpha+1}^3).$$

By adding and subtracting terms of the form  $J(S_\alpha^3 - S_{\alpha+1}^3)$  to the local Hamiltonians, we find that

$$(3.15) \quad H_L^k(\Delta^{-1}) = H_L^k(0) + \Delta^{-1}H_L^{(1)} + \left(1 - \sqrt{1 - \Delta^{-2}}\right)H_L^{(2)}$$

where

$$(3.16) \quad H_L^{(1)} = - \sum_{\alpha=-L}^{L-1} h_{\alpha,\alpha+1}^{(1)} \quad \text{with} \quad h_{\alpha,\alpha+1}^{(1)} = \frac{1}{2}(S_\alpha^+ S_{\alpha+1}^- + S_\alpha^- S_{\alpha+1}^+)$$

and

$$(3.17) \quad H_L^{(2)} = J(S_L^3 - S_{-L}^3).$$

In Theorem 3.5.3 below, we will show that both  $H_L^{(1)}$  and  $H_L^{(2)}$  are relatively bounded perturbations of  $H_L^k(0)$ . To prove such estimates, we will use the following lemma several times.

**LEMMA 3.5.1.** *Let  $A$  and  $B$  be self-adjoint  $n \times n$  matrices. If  $A \geq 0$  and  $\text{Ker}(A) \subset \text{Ker}(B)$ , then there exists a constant  $c > 0$  for which,*

$$(3.18) \quad -cA \leq B \leq cA.$$

One may take  $c = \frac{\|B\|}{\lambda_1}$  where  $\lambda_1$  denotes the smallest positive eigenvalue of  $A$ .

**Proof:** Any vector  $\psi \in \mathbb{C}^n$  can be written as  $\psi = \psi_0 + \psi_1$  where  $\psi_0 \in \text{Ker}(A)$  and  $\psi_1 \in \text{Ker}(A)^\perp$ . Clearly then,  $\lambda_1 \|\psi_1\|^2 \leq \langle \psi, A\psi \rangle$  and therefore

$$(3.19) \quad |\langle \psi, B\psi \rangle| = |\langle \psi_1, B\psi_1 \rangle| \leq \|B\| \|\psi_1\|^2 \leq \frac{\|B\|}{\lambda_1} \langle \psi, A\psi \rangle,$$

as claimed. ■

For our proof of Theorem 3.5.3, we find it useful to introduce the Ising model without boundary conditions as an auxillary Hamiltonian, i.e.,

$$H_L(0) = \sum_{\alpha=-L}^{L-1} h_{\alpha,\alpha+1}(0) \quad \text{where} \quad h_{\alpha,\alpha+1}(0) = J^2 - S_\alpha^3 S_{\alpha+1}^3.$$

It is easy to prove the next lemma.

LEMMA 3.5.2. *The Ising model without boundary terms is relatively bounded with respect to the Ising kink Hamiltonian. In particular, for any vector  $\psi$ ,*

$$\|H_L(0)\psi\| \leq \|H_L^k(0)\psi\| + 2J^2\|\psi\|.$$

**Proof:** Consider the terms of the Ising kink Hamiltonian:

$$(3.20) \quad h_{\alpha,\alpha+1}^k(0) = (J + S_\alpha^3)(J - S_{\alpha+1}^3) = h_{\alpha,\alpha+1}(0) + J(S_\alpha^3 - S_{\alpha+1}^3).$$

Summing on  $\alpha$  then, we find that

$$(3.21) \quad H_L(0) = H_L^k(0) + J(S_L^3 - S_{-L}^3),$$

and therefore, the bound

$$(3.22) \quad \|H_L(0)\psi\| \leq \|H_L^k(0)\psi\| + 2J^2\|\psi\|,$$

is clear for any vector  $\psi$ . ■

We now state the relative boundedness result.

THEOREM 3.5.3. *The linear term in the perturbation expansion of  $H_L^k(\Delta^{-1})$ , see (3.15), satisfies*

$$(3.23) \quad \left\| H_L^{(1)} \psi \right\| \leq \sqrt{J^2 + 2J^3} \|H_L^k(0)\psi\| + 2J^2 \sqrt{J^2 + 2J^3} \|\psi\|,$$

for any vector  $\psi$ . Moreover, we also have that

$$(3.24) \quad \left\| H_L^{(2)} \psi \right\| \leq 2J^2 \|\psi\|$$

**Proof:** Using Lemma 3.5.2, it is clear we need only prove that

$$(3.25) \quad \left\| H_L^{(1)} \psi \right\| \leq \sqrt{J^2 + 2J^3} \|H_L(0)\psi\|.$$

to establish (3.23). To this end, Lemma 3.5.1 provides an immediate bound on the individual terms of these Hamiltonians. In fact, observe that for any fixed  $\alpha$ , both  $h_{\alpha, \alpha+1}(0)$  and  $h_{\alpha, \alpha+1}^{(1)}$  are self-adjoint with  $h_{\alpha, \alpha+1}(0) \geq 0$  and

$$(3.26) \quad \text{Ker}(h_{\alpha, \alpha+1}(0)) = \{|\vec{m}\rangle : m_\alpha = m_{\alpha+1} = \pm J\} \subset \text{Ker}(h_{\alpha, \alpha+1}^{(1)}).$$

It is also easy to see that, for every  $\alpha$ , the first positive eigenvalue of  $h_{\alpha, \alpha+1}(0)$  is  $\lambda_1 = J$ , and we have that

$$(3.27) \quad \|h_{\alpha, \alpha+1}^{(1)}\| = \frac{1}{2} \|S_\alpha^+ S_{\alpha+1}^- + S_\alpha^- S_{\alpha+1}^+\| \leq J^2.$$

An application of Lemma 3.5.1 yields the operator inequality

$$(3.28) \quad -J h_{\alpha, \alpha+1}(0) \leq h_{\alpha, \alpha+1}^{(1)} \leq J h_{\alpha, \alpha+1}(0),$$

valid for any  $\alpha$ .

The norm bound we seek to prove will follow from considering products of these local Hamiltonians. For any vector  $\psi$ , one has that

$$(3.29) \quad \|H_L^{(1)} \psi\|^2 = \langle \psi, (H_L^{(1)})^2 \psi \rangle = \sum_{\alpha, \alpha' = -L}^{L-1} \langle \psi, h_{\alpha, \alpha+1}^{(1)} h_{\alpha', \alpha'+1}^{(1)} \psi \rangle$$

and

$$(3.30) \quad \|H_L(0)\psi\|^2 = \langle \psi, (H_L(0))^2 \psi \rangle = \sum_{\alpha, \alpha' = -L}^{L-1} \langle \psi, h_{\alpha, \alpha+1}(0) h_{\alpha', \alpha'+1}(0) \psi \rangle.$$

The arguments we provided above apply equally well to the diagonal terms of (3.29) and (3.30) in the sense that

$$(3.31) \quad -J^2 (h_{\alpha, \alpha+1}(0))^2 \leq \left( h_{\alpha, \alpha+1}^{(1)} \right)^2 \leq J^2 (h_{\alpha, \alpha}(0))^2,$$

is also valid for any  $\alpha$ . We find a similar bound by considering the terms on the right hand side of (3.29) and (3.30) for which  $|\alpha - \alpha'| > 1$ . In this case, each of the operators  $h_{\alpha, \alpha+1}(0)$  and  $h_{\alpha, \alpha+1}^{(1)}$  commute with both of the operators  $h_{\alpha', \alpha'+1}(0)$  and  $h_{\alpha', \alpha'+1}^{(1)}$ . Moreover, we conclude from (3.28) that the operators  $g_{\alpha}^{\pm} = J h_{\alpha, \alpha+1}(0) \pm h_{\alpha, \alpha+1}^{(1)}$  are non-negative for every  $\alpha$ . Since all the relevant quantities commute, it is clear that

$$(3.32) \quad 0 \leq \frac{1}{2} (g_{\alpha}^{+} g_{\alpha'}^{-} + g_{\alpha}^{-} g_{\alpha'}^{+}) = J^2 h_{\alpha, \alpha+1}(0) h_{\alpha', \alpha'+1}(0) - h_{\alpha, \alpha+1}^{(1)} h_{\alpha', \alpha'+1}^{(1)}.$$

Our observations above imply the following bound

$$(3.33) \quad \left\| H_L^{(1)} \psi \right\|^2 - J^2 \|H_L(0)\psi\|^2 \leq \sum_{\alpha = -L}^{L-2} \left\langle \psi, \left( h_{\alpha, \alpha+1}^{(1)} h_{\alpha+1, \alpha+2}^{(1)} + h_{\alpha+1, \alpha+2}^{(1)} h_{\alpha, \alpha+1}^{(1)} \right) \psi \right\rangle.$$

In fact, the terms on the right hand side of (3.33) for which either  $\alpha' = \alpha$  or  $|\alpha - \alpha'| > 1$  are non-positive by (3.31), respectively, (3.32). In the case that  $|\alpha - \alpha'| = 1$ , the operators  $h_{\alpha, \alpha+1}(0) h_{\alpha', \alpha'+1}(0)$  are non-negative (since they commute) and hence we may drop these terms; those terms that remain we group as the self-adjoint operators appearing on the right hand side of (3.33) above.

Our estimate is completed by applying Lemma 3.5.1 one more time. Note that for any  $\alpha \in \{-L, \dots, L-2\}$  the operator  $A_{\alpha} = h_{\alpha, \alpha+1}(0) + h_{\alpha+1, \alpha+2}(0)$  is self-adjoint, non-negative, and

$$(3.34) \quad \text{Ker}(A_{\alpha}) = \{ |\vec{m}\rangle : m_{\alpha} = m_{\alpha+1} = m_{\alpha+2} = \pm J \} \subset \text{Ker}(B_{\alpha}),$$

where the self-adjoint operator  $B_{\alpha}$  appearing above is given by

$$(3.35) \quad B_{\alpha} = h_{\alpha, \alpha+1}^{(1)} h_{\alpha+1, \alpha+2}^{(1)} + h_{\alpha+1, \alpha+2}^{(1)} h_{\alpha, \alpha+1}^{(1)}.$$

For each  $\alpha$ , the first positive eigenvalue of  $A_\alpha$  is  $\lambda_1(\alpha) = J$ , and it is also easy to see that  $\|B_\alpha\| \leq 2J^4$ . Thus, term by term Lemma 3.5.1 implies that

$$(3.36) \quad \langle \psi, B_\alpha \psi \rangle \leq 2J^3 \langle \psi, A_\alpha \psi \rangle,$$

from which we conclude that

$$(3.37) \quad \left\| H_L^{(1)} \psi \right\|^2 \leq (J^2 + 2J^3) \|H_L(0)\psi\|^2,$$

as claimed in (3.25). We have proved (3.23).

Equation (3.24) follows directly from the easy observation that  $\left\| H_L^{(2)} \right\|$  is equal to  $2J^2$ . ■

**3.5.2. Perturbation theory.** In Section 3.4, we verified that, in any given sector, the spectrum of the Ising kink Hamiltonian,  $H_L^k(0)$ , when restricted to the interval  $[0, 2J]$  consists of only isolated eigenvalues whose multiplicity is at most two. In fact, for the sector  $M = -2Jx + m$  these eigenvalues are determined by

$$(3.38) \quad E_\pm(m, n) = n^2 + (J \pm m)n$$

for those values of  $n \in \mathbb{N}$  with  $E_\pm(m, n) < 2J$ . It is clear from (3.38) that each of these eigenvalues have an isolation distance  $d_\pm(m, n) > 0$  from the rest of the spectrum and that this distance is independent of the length scale  $L$ .

For our proof of the relative boundedness result in Theorem 3.5.3, we expanded the Hamiltonian as

$$(3.39) \quad H_L^k(\Delta^{-1}) = H_L^k(0) + \Delta^{-1} H_L^{(1)} + \left(1 - \sqrt{1 - \Delta^{-2}}\right) H_L^{(2)}.$$

Using the first resolvent formula, it is easy to see that

$$(3.40) \quad \left( H_L^k(\Delta^{-1}) - \xi \right)^{-1} = R(\xi) \left[ 1 + \left( \Delta^{-1} H_L^{(1)} + \left(1 - \sqrt{1 - \Delta^{-2}}\right) H_L^{(2)} \right) R(\xi) \right]^{-1},$$

where we have denoted the resolvent by  $R(\xi) = \left( H_L^k(0) - \xi \right)^{-1}$ , and it is assumed that  $\Delta^{-1}$  has been chosen small enough so that

$$(3.41) \quad \left\| \left( \Delta^{-1} H_L^{(1)} + \left(1 - \sqrt{1 - \Delta^{-2}}\right) H_L^{(2)} \right) R(\xi) \right\| < 1.$$

It is clear from sections II.1.3-4 of [Kat82] and chapter I of [SR72] that the spectral projections corresponding to  $H_L^k(\Delta^{-1})$  can be written as a power series in  $\Delta^{-1}$ , the coefficients of which being integrals of the resolvent over a fixed contour  $\Gamma$ . Proving an estimate of the form (3.41) for  $\Delta$  large enough, uniformly with respect to  $\xi \in \Gamma$ , is sufficient to guarantee analyticity of the spectral projections. We verify such a uniform estimate below.

Let  $E_{\pm}(m, n)$  be an eigenvalue of  $H_L^k(0)$  with isolation distance  $d_{\pm}(m, n)$  as specified above. Denote by  $\Gamma$  the circle in the complex plane centered at  $E_{\pm}(m, n)$  with radius  $d_{\pm}(m, n)/2$ . We claim that if

$$(3.42) \quad \Delta > 18J^{5/2},$$

then (3.41) is satisfied uniformly for  $\xi \in \Gamma$ .

We proved in Theorem 3.5.3 that for any vector  $\psi$ ,

$$(3.43) \quad \left\| H_L^{(1)} \psi \right\| \leq \sqrt{J^2 + 2J^3} \|H_L^k(0)\psi\| + 2J^2 \sqrt{J^2 + 2J^3} \|\psi\|.$$

Applying this bound to vectors  $\psi$  of the form  $\psi = R(\xi)\phi$  yields a norm estimate on  $H_L^{(1)}R(\xi)$ , i.e.,

$$(3.44) \quad \left\| H_L^{(1)}R(\xi)\phi \right\| \leq \left( \sqrt{J^2 + 2J^3} \|H_L^k(0)R(\xi)\| + 2J^2 \sqrt{J^2 + 2J^3} \|R(\xi)\| \right) \|\phi\|.$$

Moreover, since

$$(3.45) \quad \|H_L^k(0)R(\xi)\| \leq 1 + |\xi| \|R(\xi)\|,$$

we have proved that

$$(3.46) \quad \left\| \Delta^{-1} H_L^{(1)} R(\xi) \right\| \leq \Delta^{-1} \sqrt{J^2 + 2J^3} [1 + (|\xi| + 2J^2) \|R(\xi)\|].$$

Similar arguments, again using Theorem 3.5.3, imply that

$$(3.47) \quad \left\| \left(1 - \sqrt{1 - \Delta^{-2}}\right) H_L^{(2)} R(\xi) \right\| \leq \left(1 - \sqrt{1 - \Delta^{-2}}\right) 2J^2 \|R(\xi)\|.$$

For  $\xi \in \Gamma$ , the circular contour described above, we have that

$$(3.48) \quad \|R(\xi)\| = \frac{1}{\text{dist}(\xi, \sigma(H_L^k(0)))} = \frac{2}{d_{\pm}(m, n)},$$

and

$$(3.49) \quad |\xi| \leq E_{\pm}(m, n) + d_{\pm}(m, n)/2.$$

We derive a bound of the form (3.41), uniform for  $\xi \in \Gamma$ , by ensuring  $\Delta$  large enough so that

$$(3.50) \quad C_1 \Delta^{-1} + C_2(1 - \sqrt{1 - \Delta^{-2}}) < 1,$$

where

$$(3.51) \quad C_1 = \sqrt{J^2 + 2J^3} \left[ 1 + \left( \frac{2E_{\pm}(m, n)}{d_{\pm}(m, n)} + 1 + \frac{4J^2}{d_{\pm}(m, n)} \right) \right] \quad \text{and} \quad C_2 = \frac{4J^2}{d_{\pm}(m, n)}.$$

Explicitly, one finds that the inequality (3.50) is satisfied for all

$$(3.52) \quad \Delta > \frac{C_1^2 + C_2^2}{C_2 \sqrt{C_1^2 + 2C_2 - 1} + C_1 - C_1 C_2}$$

Equation (3.42) is a simple sufficient condition for  $\Delta$  to satisfy this inequality. This is easy to verify if one first replaces  $1 - \sqrt{1 - \Delta^{-2}}$  by  $\Delta^{-2}$  in (3.50).

## CHAPTER 4

## Implementing gates

## 4.1. Introduction

In this chapter<sup>1</sup> we study the implementation of quantum gates using the ferromagnetic XXZ spin chain with kink boundary conditions. For quantum computers to become a reality we need to find or build physical systems that faithfully implement the quantum gates used in the algorithms of quantum computation. The basic requirement is that the experimenter has access to two states of a quantum system that can be effectively decoupled from environmental noise for a sufficiently long time, and that transitions between these two states can be controlled to simulate a number of elementary quantum gates (unitary transformations). Systems that have been investigated intensively are atomic levels in ion traps [CZ95, MMK<sup>+</sup>95], superconducting device physics using Josephson rings [MOL<sup>+</sup>99], nuclear spins [CVZ<sup>+</sup>98] (using NMR in suitable molecules) and quantum dots [LD95]. In this paper we demonstrate the implementation of quantum gates using one-dimensional spin- $J$  systems. The results are obtained using a computer simulation of these systems.

The Hamiltonian of the XXZ model with kink boundary conditions is given by

$$(4.1) \quad H_L^k(\Delta^{-1}) = \sum_{\alpha=-L+1}^{L-1} \left[ (J^2 - S_\alpha^3 S_{\alpha+1}^3) - \Delta^{-1} (S_\alpha^1 S_{\alpha+1}^1 + S_\alpha^2 S_{\alpha+1}^2) \right] + J \sqrt{1 - \Delta^{-2}} (S_{-L+1}^3 - S_L^3)$$

where  $S_\alpha^1$ ,  $S_\alpha^2$  and  $S_\alpha^3$  are the spin- $J$  matrices acting on the site  $\alpha$ . Apart from the magnitude of the spins,  $J$ , the main parameter of the model is the anisotropy  $\Delta > 1$  and the limit  $\Delta \rightarrow \infty$  is referred to as the *Ising limit*. In the case of  $J = 1/2$  kink boundary conditions were first introduced in [PS90]. They lead to ground states with a domain wall between down spins on the left portion of the chain and up spins on the right. The third component of the magnetization,  $M$ , is conserved, and there is exactly one ground state for each value

---

<sup>1</sup>The text of this chapter is essentially a reprint of the paper *arXiv:0902.1276*

of  $M$ . Different values of  $M$  correspond to different positions of the domain walls, which in one dimension are sometimes referred to as kinks. In [KNS01], Koma, Nachtergaele, and Starr showed that there is a spectral gap above each of the ground states in this model for all values of  $J$ . Recently [MNSS08] it was shown that for spin values  $J \geq \frac{3}{2}$  and for sufficiently large value of the anisotropy  $\Delta$  the low lying spectrum of (4.1) for each value of  $M$  has isolated eigenvalues that persist in the thermodynamic limit.

The presence of isolated eigenvalues is ideal from the point of view of quantum computation. The idea is to use the subspace, denoted by  $\mathcal{D}$ , of the ground state and the first excited state of the Hamiltonian to encode a qubit. In the absence of noise (coupling to the environment), states corresponding to eigenvalues have an infinite life time. Generically, when the eigenvalues are embedded in a continuum, arbitrarily small perturbations will turn them into resonances, i.e., states with a finite life time. By using a subspace of states corresponding to isolated eigenvalues, we can expect much larger life times even in the presence of noise. Heuristically, there is an energy barrier protecting the states from decaying. Since the eigenvalues are *not* protected by a topological invariant, it is possible to use local, finite-strength perturbations to control transitions in the system. In principle, such perturbations may be implemented in a suitable solid state setup.

Concretely the idea is to let the system evolve under its own unitary time evolution generated by the Hamiltonian (4.1) with the addition of a few local control fields. We have two requirements to fulfill: the time evolution should leave the qubit space  $\mathcal{D}$  approximately invariant, and the (approximately) unitary matrix describing the dynamics restricted to  $\mathcal{D}$  and stopped at a suitable time should coincide with the desired quantum gate.

The control inputs needed to drive the system such that high fidelity gates are obtained are determined using techniques from optimal control theory. The simulation of the time evolution of the chain that is large enough to resemble the properties in the thermodynamic limit is carried out using the Density Matrix Renormalization Group (DMRG) algorithm. Figure 4.1 shows the transition of the magnetic profiles in the z-direction from the ground to the first excited state using the Not gate constructed from a spin- $\frac{3}{2}$  XXZ spin chain of length 50 sites. We also demonstrate the construction of Pi-8, Hadamard, and Phase gates that form a set of universal single qubit gates.

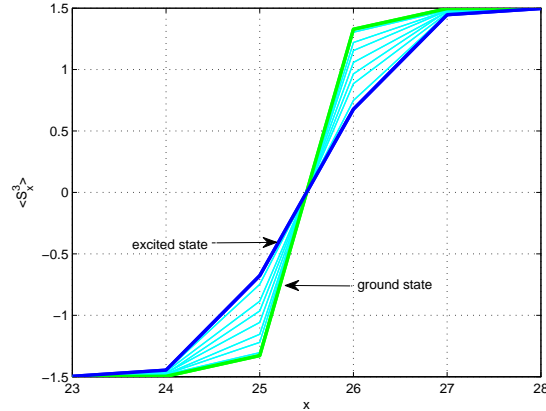


FIGURE 4.1. The transitioning of the magnetization profile from the ground to the first excited state using a Not gate. Simulation obtained for a chain of 50 ( $L=25$ ) sites using DMRG with  $\Delta^{-1} = 0.3$  and  $M = 0$ . The lines in between the ground and excited state profiles represent the profile at intermediate times between  $t = 0$  and the gate time  $T = 20$ .

In order to have a viable quantum computing scheme one needs to implement at least one 2-qubit gate. Here we have implemented the C-Not gate which, in combination with the 1-qubit gates, is known to be universal [Be95].

Our scheme capitalizes on the kink nature of the excitations of the XXZ Hamiltonian, which are rather sharply localized. We imagine a setup with two parallel chains with the location of the kink lined up in their ground states. The subspace for the 2-qubit state space is then  $\mathcal{D}_1 \otimes \mathcal{D}_2$ , where  $\mathcal{D}_1$  represents the space of isolated eigenvalues of the first chain and  $\mathcal{D}_2$  for the second chain. A set of three controls localized near the kinks is used to generate the single qubit gates acting on  $\mathcal{D}_1$  and  $\mathcal{D}_2$  and a C-Not gate on  $\mathcal{D}_1 \otimes \mathcal{D}_2$ . This scheme produces a universal set of gates necessary for two-qubit computation. It is clear how to generalize this scheme to implement  $n$ -qubit computation. Since a universal set of single qubit gates and nearest neighbor C-Not gates are universal for  $n$ -qubit computation, this can be achieved by using  $n$  parallel chains and controls that are localized and act on neighboring chains only.

In the next section we describe the model and review some of the past results. Then, in section 4.2, the optimal control problem to construct the quantum gates is described. Section 4.3 is devoted to the DMRG algorithm and the specific adaptations to the XXZ

spin chain. Finally, in section 4.4 we present our results based on numerical simulations of the XXZ Hamiltonian using the DMRG algorithm.

## 4.2. Quantum gates using quantum control

The problem of constructing quantum gates can be formulated as a problem in quantum control theory [MK05]. The goal is to steer the system using a small number of control parameters such that the unitary operator describing the quantum dynamics after a finite time  $T$ , has maximal overlap with a desired target unitary (the gate). From a control perspective these problems reduce to control of bilinear systems evolving on finite dimensional Lie groups. This is an optimal control problem on a two-level system which has been studied widely with exact results known in some cases. For example, time optimal implementation of single and two qubit quantum gates was studied [KBG01] when the Lie algebra  $\mathfrak{g}$  of  $su(2)$  ( $su(4)$ ) can be decomposed as a Cartan pair  $\mathfrak{g} = \mathfrak{k} \oplus \mathfrak{p}$  with  $\mathfrak{k}$  is the Lie subalgebra generated by the drift Hamiltonian and  $\mathfrak{p}$  is the Lie sub algebra generated by the control Hamiltonian's. Finding the time optimal trajectories is reduced to finding geodesics on the coset space  $G/K$  ( $G$  and  $K$  being the Lie Groups corresponding to  $\mathfrak{g}$  and  $\mathfrak{k}$ ). The problem of driving the evolution operator while minimizing an energy-type quadratic cost was studied in [DD01]. In this case the optimal solutions can be expressed as Elliptic functions. The time optimal problem of population transfer problem of a two-level quantum system and bounded controls was studied in [BM05] and again explicit expressions for the optimal trajectories. In this paper we follow a numerical gradient based approach to optimal control [D'A08, KRK<sup>+</sup>05].

**4.2.1. Single qubit gates.** We consider the problem of time evolution of the one-dimensional XXZ chain under external controls. The equation of motion for the unitary evolution of the XXZ chain isolated from the environment is given by Schrödinger's equation

$$(4.2) \quad \dot{U}(t) = -i \left( H_L^k(\Delta^{-1}) + v(t) H^{\text{ext}} \right) U, \quad U(0) = \mathbb{1}$$

In control terminology  $H_L^k(\Delta^{-1})$  is the free or drift Hamiltonian and  $H^{\text{ext}}$  is the control Hamiltonian corresponding to the control field  $v(t)$ . We require that  $\mathcal{D}$  is an invariant subspace of  $H^{\text{ext}}$ , so that the time evolution of the system 4.2 given by the unitary  $U(t)$  starting from an initial state in  $\mathcal{D}$  will be constrained to  $\mathcal{D}$  at all future times. The induced

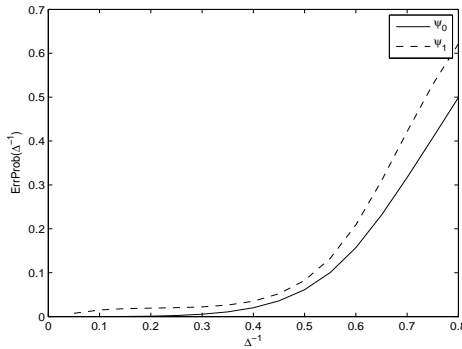


FIGURE 4.2. ErrProb, defined in (4.4), as a function of  $\Delta^{-1}$ , calculated for the ground and first excited state  $\psi_0$  and  $\psi_1$ , with  $H^{\text{ext}} = S_0^3 S_1^3$ . This quantity provides a measure of the escape rate out of the qubit subspace.

evolution on  $\mathcal{D}$  at any specified final time  $T$  will be the quantum gate on the qubit space  $\mathcal{D}$  and is given by the 2x2 matrix

$$(4.3) \quad (U_{xxz})_{ij} := \langle \psi_i | U(T) | \psi_j \rangle \quad i = 0, 1$$

The control Hamiltonian we choose is the two site operator  $H^{\text{ext}} = S_0^3 S_1^3$ . In practice for  $S_0^3 S_1^3$  there is a very small error probability for states to move out of  $\mathcal{D}$  and the matrix  $U_{xxz}$  is not exactly unitary. The matrix elements  $\langle \psi_0 | H^{\text{ext}} | \psi_k \rangle$  and  $\langle \psi_1 | H^{\text{ext}} | \psi_k \rangle$   $k \neq 0, 1$  are proportional to the transition probabilities to move from states  $\psi_0$  and  $\psi_1$  to other eigenstates of  $H_L^k(\Delta^{-1})$ . We calculate the error probability to move out of the subspace  $\mathcal{D}$  by the following estimates of these matrix elements

$$(4.4) \quad \text{ErrProb} = \|H^{\text{ext}}\psi_i\|^2 - |\langle \psi_0 | H^{\text{ext}} \psi_i \rangle|^2 - |\langle \psi_1 | H^{\text{ext}} \psi_i \rangle|^2$$

for  $i = 0, 1$ . Figure 4.2 shows that the probabilities of transitioning out of the subspace  $\mathcal{D}$  are extremely small for  $\Delta^{-1} \leq 0.3$ .

**4.2.2. Implementing two-qubit gates.** The idea for implementing two-qubit gates is to use two copies of the XXZ chain. The Hilbert space for two-qubit quantum computation is  $\mathcal{D}_1 \otimes \mathcal{D}_2 \cong \mathbb{C}^4$ , where  $\mathcal{D}_1$  and  $\mathcal{D}_2$  are the subspaces spanned by the ground state and first excited state of the first chain and second chain respectively. The Hamiltonian of an

uncoupled two chain system is given by

$$H_L^k(\Delta^{-1})^{(1,2)} := H_L^k(\Delta^{-1})^{(1)} + H_L^k(\Delta^{-1})^{(2)}$$

Here the notation  $H_L^k(\Delta^{-1})^{(1)}$  is to be interpreted as  $\underbrace{H_L^k(\Delta^{-1})}_{\text{chain1}} \otimes (\mathbb{I} \otimes \cdots \otimes \mathbb{I})_{\text{chain2}}$  and  $H_L^k(\Delta^{-1})^{(2)}$  is to be interpreted as  $(\mathbb{I} \otimes \cdots \otimes \mathbb{I})_{\text{chain1}} \otimes \underbrace{H_L^k(\Delta^{-1})}_{\text{chain2}}$ . The two-qubit space is spanned by the four vectors  $\psi_{mn} := \psi_m \otimes \psi_n$  for  $m, n = 0, 1$  which are eigenvectors of the above Hamiltonian. If we consider the control system

$$(4.5) \quad \dot{U} = -i \left( H_L^k(\Delta^{-1})^{(1,2)} + v_1(t)(S_0^3 S_1^3)^{(1)} + v_2(t)(S_0^3 S_1^3)^{(2)} \right)$$

with  $U(0) = \mathbb{I}$ , then by selectively turning on  $v_1(t)$  and  $v_2(t)$  for certain time periods, the above system is equivalent to the control system (4.2) on chains 1 and 2 respectively during those time intervals. This can be used to generate single qubit gates on  $\mathcal{D}_1$  and  $\mathcal{D}_2$ . Moreover by simultaneously using  $v_1(t)$  and  $v_2(t)$  the local gates i.e. gates of the kind  $X_1 \otimes Y_2$  can be generated on  $\mathcal{D}_1 \otimes \mathcal{D}_2$ . To implement a two-qubit quantum computing scheme we need to also implement perfectly entangling gates i.e. a gate that can take a product state to a maximally entangled state. It is known that single qubit gates and any perfectly entangling gate are universal for two-qubit quantum computing [ZVSW03]. Clearly such a gate cannot be implemented by the control scheme (4.5) alone. In this paper we choose to implement the C-Not gate, which is an example of a perfectly entangling gate. For this purpose we make use of an additional control namely  $(S_0^3 S_1^3)^{(1)} \otimes (S_0^3 S_1^3)^{(2)}$ .

We demonstrate the C-Not gate to high precision by using following control system

$$(4.6) \quad \dot{U} = -i \left( H_L^k(\Delta^{-1})^{(1,2)} + v_1(t)(S_0^3 S_1^3)^{(1)} + v_2(t)(S_0^3 S_1^3)^{(2)} \right. \\ \left. + v_3(t)(S_0^3 S_1^3)^{(1)} \otimes (S_0^3 S_1^3)^{(2)} \right)$$

with  $U(0) = \mathbb{I}$  by selectively turning on and off some or all of the control fields  $v_1(t)$ ,  $v_2(t)$  and  $v_3(t)$  for specified time periods. Figure 4.3 shows a diagrammatic representation of the two-qubit scheme. The C-Not gate is then given by the  $4 \times 4$  matrix with elements

$$(\text{C-Not}^{xxz})_{mn;rs} := \langle \psi_{mn} | U(T) | \psi_{rs} \rangle \quad i = 0, 1$$

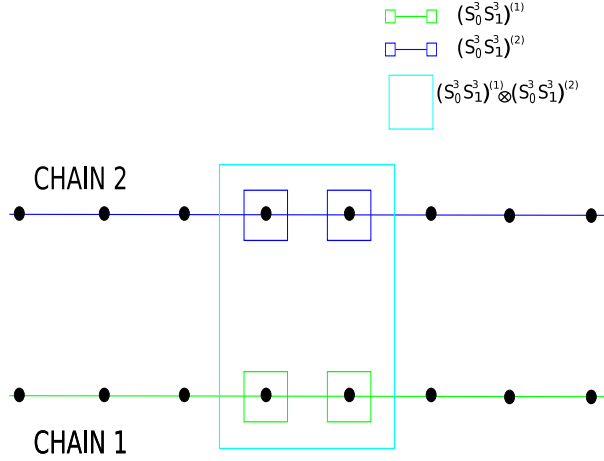


FIGURE 4.3. Configuration of two XXZ chains showing the localized controls required to implement the C-Not gate.

**4.2.3. Optimal control.** We first solve the control problems (4.2) and (4.6) for the projected system on  $\mathcal{D}$  for the single chain and  $\mathcal{D}_1 \otimes \mathcal{D}_2$  for two chain system.

$$(4.7) \quad \dot{U}(t) = -i \left( H + \sum_k v_k(t) B_k \right) U, \quad U(0) = \mathbb{I}$$

For the projected system on  $\mathcal{D}$  the  $H$  and  $B_k$ 's are given by the  $2 \times 2$  matrices

$$(4.8) \quad \begin{aligned} H_{ij} &= \langle \psi_i | H_L^k(\Delta^{-1}) | \psi_j \rangle \\ (B_1)_{ij} &= \langle \psi_i | H_L^k(\Delta^{-1}) | \psi_j \rangle, \quad i, j = 0, 1 \end{aligned}$$

whereas the the projected system on  $\mathcal{D}_1 \otimes \mathcal{D}_2$  the control problem involves  $4 \times 4$  matrices

$$(4.9) \quad \begin{aligned} H_{mn;rs} &= \langle \psi_{mn} | H_L^k(\Delta^{-1})^{(1,2)} | \psi_{rs} \rangle \\ (B_1)_{mn;rs} &= \langle \psi_{mn} | (S_0^3 \cdot S_1^3)^{(1)} | \psi_{rs} \rangle \\ (B_2)_{mn;rs} &= \langle \psi_{mn} | (S_0^3 \cdot S_1^3)^{(2)} | \psi_{rs} \rangle \\ (B_3)_{mn;rs} &= \langle \psi_{mn} | (S_0^3 \cdot S_1^3)^{(1)} \otimes (S_0^3 \cdot S_1^3)^{(2)} | \psi_{rs} \rangle \end{aligned}$$

where  $m, n, r, s = 0, 1$ . The overlap between a desired unitary gate  $U_f$  and the solution of (4.6) at time  $T$ ,  $U(T)$ , is measured as the difference in the norm square  $\|U_f - U(T)\|^2$ , and the norm is defined in terms of the standard inner product  $\langle V | W \rangle := \text{Tr}(V^\dagger W)$ . The norm

can be written as

$$\|U_f - U(T)\|^2 = \|U_f\|^2 - 2\text{Re}\langle U_f|U(T)\rangle + \|U(T)\|^2$$

and hence minimizing this norm is equivalent to maximizing

$$(4.10) \quad \Phi := \text{Re}\langle U_f|U(T)\rangle = \text{Tr}(U_f^\dagger U(T))$$

We define the gate fidelity as

$$(4.11) \quad \mathcal{F}_{\text{Gate}} := \frac{|\text{Tr}(U_f^\dagger U(T))|}{\text{Tr}(\mathbb{I})}$$

To select the optimal control fields  $v_i(t)$  we use the numerical gradient ascent approach described in many books on control theory. This approach was applied to the quantum setting in [KRK<sup>+</sup>05]. We start with the necessary conditions for optimality called the Pontryagin maximum principle which is a generalization of the Euler-Lagrange equations from calculus of variations. In the problems with costs of type (4.10) and no a priori bound on controls, Pontryagin's maximum principle takes the following form

**THEOREM 4.2.1.** (*Pontryagin maximum principle [KRK<sup>+</sup>05, BL07]*) *If  $v_i(t)$ 's are optimal controls of the system (4.6) and  $U(t)$  the corresponding trajectory solution, then there exists a nonzero operator valued Lagrange multiplier  $\lambda$  which is the solution of the adjoint equations*

$$\begin{aligned} \dot{\lambda}(t) &= -iH(t)\lambda(t) && \text{with terminal condition} \\ \lambda'(T) &= -\frac{\partial\Phi(T)}{\partial U(T)} = -U_f \end{aligned}$$

and a scalar valued Hamiltonian function  $h(U(t), v_i(t)) := \text{Re Tr}(-i\lambda'(t)H(t)U(t))$  such that, for every  $\tau \in (0, T]$  we have

$$(4.12) \quad \frac{\partial h(U)}{\partial v_i} = \text{Im Tr}(\lambda'(t)B_i U(t)) = 0$$

The algorithm to find the optimal controls is as follows

- (1) A suitable gate time  $T$  is chosen and discretized in  $N$  equal steps of duration  $\Delta t = \frac{T}{N}$ . The initial control  $v_i^{(0)}(t_k)$  for all the discretized time intervals is based on a guess or at random.
- (2) For these piecewise constant controls, from  $U(0) = \mathbb{1}$  and  $\lambda(T) = -U_f$ , compute the forward and backward propagation respectively as follows

$$(4.13) \quad U^{(r)}(t_k) = F^{(r)}(t_k)F^{(r)}(t_{k-1}) \dots F^{(r)}(t_1)$$

$$(4.14) \quad \lambda^{(r)}(t_k) = F^{(r)}(t_k)F^{(r)}(t_{k+1}) \dots F^{(r)}(t_N)\lambda(T)$$

for all  $t_1, \dots, t_N$  and where  $r$  is an iteration number of the algorithm initially set to 0 and

$$F^{(r)}(t_k) = \exp\left\{-i\Delta t\left(H + \sum_i v_i^{(r)}(t_k)B_i\right)\right\}$$

- (3) Substitute the equations (4.13) and (4.14) into equation (4.12) to evaluate the gradient, and then update the controls as

$$v_i^{(r+1)}(t_k) = v_i^{(r)}(t_k) + \tau \frac{\partial h(U(t_k), v_i(t_k))}{\partial v_i}$$

where  $\tau$  is a small step size.

- (4) if  $\mathcal{F}_{Gate} < \gamma$  ( $\gamma$  being the level of accuracy) then done, otherwise goto step (2) for the next iteration with the updated controls.

Having solved the control problem on the projected systems to get the optimal controls  $v_1(t)$ ,  $v_2(t)$  and  $v_3(t)$  we would like to apply them to a large system and see their effects on the projected system. However simulating even a moderately sized spin chain is hard because of the exponentially growing dimension of the Hilbert space. In the next section we describe an algorithm by which we are able to simulate the XXZ chain of 50 sites.

### 4.3. DMRG simulations for quantum gates

To see the effect of the evolution of the XXZ chain with external magnetic controls we numerically simulate the XXZ chain using the DMRG algorithm. The dynamics of the interfaces of the XXZ chain using DMRG was studied recently in [MNS08]. The standard DMRG algorithm is a numerical algorithm originally developed by Steven White [Whi93] that has worked successfully in providing very accurate results for ground state energies

and correlation functions in strongly correlated systems. Modifications to this method [Vid04, WF04] allow to address the physics of time-dependent and out of equilibrium systems. The crux of the DMRG algorithm is a decimation procedure that chooses the physically most relevant states to describe the target states. It is now known that DMRG works well because the ground states of non-critical quantum chains like the XXZ chain are only slightly entangled, i.e. they obey an area law of entanglement that says that the entanglement between a distinguished block of the chain and the rest of the chain is bounded by the boundary area of the block. In fact the DMRG procedure is a variational ansatz over states known as Matrix product states (MPS) [FNV92]. The standard DMRG procedure and its connection with MPS and entanglement is described in detail in [Sch05]. For a single XXZ chain our target states are the ground state  $\psi_0$  and first excited state  $\psi_1$  restricted to a sector of magnetization. We use the standard DMRG procedure with the adaptation that we grow the chain while restricting the blocks to the sector of zero magnetization using the symmetry of the Hamiltonian (see [MNS08]).

For the two-qubit gates we convert the two chain system to a one dimensional spin chain by a spin ladder construction.

$$\begin{aligned} \mathcal{H}_{-L+1}^{(1)} \otimes \mathcal{H}_{-L+2}^{(1)} \otimes \dots \otimes \mathcal{H}_L^{(1)} &= \mathcal{H}_{[-L+1,L]}^{(1)} \\ \otimes & \quad \quad \quad \otimes & \quad \quad \quad \otimes & \quad \quad \quad \otimes \\ \mathcal{H}_{-L+1}^{(2)} \otimes \mathcal{H}_{-L+2}^{(2)} \otimes \dots \otimes \mathcal{H}_L^{(2)} &= \mathcal{H}_{[-L+1,L]}^{(2)} \end{aligned}$$

The single site Hilbert space for the DMRG is the rung composed of  $\mathcal{H}_\alpha^{(1)} \otimes \mathcal{H}_\alpha^{(2)}$  for  $\alpha \in [-L+1..L]$ . On this site we define the local operators

$$S_\alpha^{i(1)} = S_\alpha^i \otimes \mathbb{1}_\alpha, \quad S_\alpha^{i(2)} = \mathbb{1}_\alpha \otimes S_\alpha^i \quad \text{for } i = 1, 2, 3$$

We can then write the Hamiltonian of this single chain using the above construction

$$(4.15) \quad H_L^k(\Delta^{-1})^{(1,2)} := \sum_{\alpha=-L+1}^{L-1} h_{\alpha,\alpha+1}^{(1)}(\Delta^{-1}) + h_{\alpha,\alpha+1}^{(2)}(\Delta^{-1})$$

$$(4.16) \quad \begin{aligned} h_{\alpha,\alpha+1}^{(k)}(\Delta^{-1}) &= J^2 - S_\alpha^{3(k)} S_{\alpha+1}^{3(k)} - \Delta^{-1} (S_\alpha^{1(k)} S_{\alpha+1}^{1(k)} \\ &\quad + S_\alpha^{2(k)} S_{\alpha+1}^{2(k)}) + J \sqrt{1 - \Delta^{-2}} (S_\alpha^{3(k)} - S_{\alpha+1}^{3(k)}) \end{aligned}$$

for  $k = 1, 2$ . We carry out the DMRG procedure as described in the algorithm with the Hamiltonian  $H_L^k(\Delta^{-1})^{(1,2)}$  but we ensure that we keep both the chains in the magnetization sector 0 by simultaneously diagonalizing  $H_L^k(\Delta^{-1})^{(1,2)}$  with the total magnetization operators

$$S_{tot}^{(k)} = \sum_{\alpha=-L+1}^L S_{\alpha}^{3(k)} \quad \text{for } k = 1, 2$$

The target states  $\psi_0 \otimes \psi_0$ ,  $\psi_0 \otimes \psi_1$ ,  $\psi_1 \otimes \psi_0$ ,  $\psi_1 \otimes \psi_1$  are the simultaneous eigenvectors of these operators and form the computational basis  $|00\rangle$ ,  $|01\rangle$ ,  $|10\rangle$  and  $|11\rangle$  for two-qubit quantum computation.

To compute the time evolution of the chain under the controlled evolution by the external fields we use the time-dependent DMRG procedure. The idea is that a two site operator can be applied to a DMRG state most effectively by expressing the state in the basis where the left block has length  $x - 1$  so the two middle sites that are untruncated are the sites where the operator is acting. We can write the time evolution in the Trotter decomposition

$$(4.17) \quad e^{-iH\delta} \cong e^{-\frac{i}{2}h_{-L+1,-L+2}} e^{-\frac{i}{2}h_{-L+2,-L+3}} \dots e^{-\frac{i}{2}h_{L-2,L-1}} e^{-\frac{i}{2}h_{L-1,L}} + O(\delta^3)$$

To apply  $e^{-iH\delta}$  to the ground and excited states in the basis with the center sites all the way to the left we apply  $e^{-\frac{i}{2}h_{-L+1,-L+2}}$ . After shifting one site to the right we apply  $e^{-\frac{i}{2}h_{-L+2,-L+3}}$  etc. Since all our controls are two site controls at the center, only the interaction  $h_{0,1}$  is time-dependent. In the adaptive time-dependent methods the Hilbert space is continuously modified as time progresses by carrying out reduced basis transformations on the evolved state. In our case since the gates are obtained in a relatively short period of time our Hilbert space remains unchanged resembling the static DMRG methods.

#### 4.4. Results

In this section we present numerical results of the construction of quantum gates using the spin-3/2 XXZ spin chain. Our results are for the universal set of single qubit gates consisting of the Not (X), Hadamard (H), Pi-8 (T) and Phase (S) gates and the two-qubit C-Not gate. All results are obtained using the DMRG algorithm and the optimal control methods described in the previous sections. The steps carried out to obtain the single qubit gates are as follows

- (1) We use ground state DMRG of the XXZ chain to obtain the lowest eigenvectors  $\psi_0$  and  $\psi_1$  of  $H_L^k(\Delta^{-1})$  in the sector corresponding to  $M = 0$ .
- (2) We obtain the projected  $2 \times 2$  control system of equation (4.7) with matrices  $H$  and  $B_1$  with matrix elements given by (4.8). For a target gate  $U_f$  and a suitable final time  $T$  we find the optimal control  $v_1(t)$  on this  $2 \times 2$  system using the technique described in section 4.2.3.
- (3) Finally we apply the time-dependent DMRG procedure of section 4.3 to the chain of (4.2) for a specified time  $T$  starting from  $\psi_0$  and  $\psi_1$  and using the  $v_1(t)$  found in step 2 to get the time evolved states  $\psi_0(T) = U(T)\psi_0$  and  $\psi_1(T) = U(T)\psi_1$ . We compute the induced evolution on the subspace  $\mathcal{D}$  to obtain the gate  $U_{xxz}$  given by the matrix elements  $\langle \psi_i | \psi_j(T) \rangle$  for  $i, j = 0, 1$  and compare the overlap with  $U_f$  using equation (4.11).

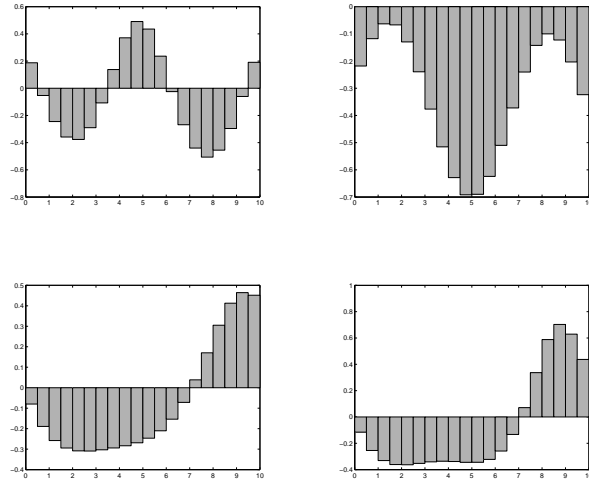


FIGURE 4.4. (Clockwise) The controls for Not, Hadamard, Pi-8 and Phase gates controls plotted versus time discretized for time steps of  $\Delta t = 0.5$ .

Our desired single qubit target gates are given by the unitaries.

$$X = \begin{pmatrix} 0 & i \\ i & 0 \end{pmatrix} \quad H = \frac{1}{\sqrt{2}} \begin{pmatrix} i & i \\ i & -i \end{pmatrix} \quad T = \begin{pmatrix} e^{-i\pi/4} & 0 \\ 0 & e^{-i\pi/4} \end{pmatrix} \quad S = \begin{pmatrix} e^{-i\pi/8} & 0 \\ 0 & e^{-i\pi/8} \end{pmatrix}$$

TABLE 4.1. Numerical simulation of the construction of the Not, Pi-8, Hadamard and Phase gates. Results are obtained using DMRG and time-dependent DMRG for a spin- $\frac{3}{2}$  chain of  $L = 50$  sites and at  $\Delta^{-1} = 0.3$  in the sector corresponding to  $M = 0$ . The table shows the values of the control field  $v_1(t)$  with gate time  $T = 10$  discretized with  $\Delta t = 0.5$ .

Not(X)	Hadamard(H)	Pi-8(T)	Phase(S)
0.1874	-0.2182	-0.1152	-0.0797
-0.0533	-0.1176	-0.2544	-0.1889
-0.2447	-0.0631	-0.3310	-0.2579
-0.3587	-0.0670	-0.3613	-0.2945
-0.3764	-0.1296	-0.3632	-0.3085
-0.2901	-0.2396	-0.3524	-0.3091
-0.1075	-0.3766	-0.3410	-0.3031
0.1376	-0.5154	-0.3358	-0.2943
0.3712	-0.6286	-0.3383	-0.2836
0.4908	-0.6917	-0.3443	-0.2691
0.4355	-0.6899	-0.3441	-0.2466
0.2359	-0.6241	-0.3222	-0.2103
-0.0246	-0.5099	-0.2590	-0.1538
-0.2681	-0.3723	-0.1328	-0.0715
-0.4399	-0.2404	0.0709	0.0386
-0.5065	-0.1424	0.3368	0.1704
-0.4553	-0.1001	0.5877	0.3053
-0.2959	-0.1225	0.7029	0.4128
-0.0605	-0.2033	0.6294	0.4642
0.1909	-0.3236	0.4374	0.4516

The gates obtained using the XXZ chain and their fidelities are as follows. The optimal controls  $v_1(t)$  used to get the gate results are shown in Figure 4.4 and Table 4.1.

$$X_{xxz} = \begin{pmatrix} 0.0016 - 0.0011i & 0.0033 + 0.9997i \\ -0.0017 + 0.9997i & 0.0017 + 0.0011i \end{pmatrix} \quad \mathcal{F}_X = 0.9997,$$

$$H_{xxz} = \begin{pmatrix} -0.0027 + 0.7081i & 0.0011 + 0.7053i \\ -0.0016 + 0.7052i & -0.0022 - 0.7085i \end{pmatrix} \quad \mathcal{F}_H = 0.9995,$$

$$T_{xxz} = \begin{pmatrix} 0.9221 - 0.3859i & -0.0037 + 0.0038i \\ 0.0037 + 0.0038i & 0.9216 + 0.3871i \end{pmatrix} \quad \mathcal{F}_T = 0.9995,$$

$$S_{xxz} = \begin{pmatrix} 0.7043 - 0.7095i & -0.0046 + 0.0015i \\ 0.0045 + 0.0016i & 0.7017 + 0.7121i \end{pmatrix} \quad \mathcal{F}_S = 0.9997$$

For the C-Not gate the procedure described earlier is only slightly modified. We do the ground state DMRG of a one dimensional chain built from the spin ladder described in section 4.3 to get four eigenvectors  $\psi_{mn}$  for  $m, n = 0, 1$ . The optimal control procedure is applied to the  $4 \times 4$  control system (4.7) with  $H, B_1, B_2, B_3$  given by equations (4.9) to find the controls  $v_1(t), v_2(t)$  and  $v_3(t)$ . The time-dependent DMRG procedure is applied to the chain of equation (4.6) for time  $T$  with the controls  $v_1(t), v_2(t)$  and  $v_3(t)$  to get the time evolved states  $\psi_{mn}(T) = U(T)\psi_{mn}$ . The induced evolution on the subspace  $\mathcal{D}_1 \otimes \mathcal{D}_2$  gives the C – Not<sub>xxz</sub> gate with matrix elements  $\langle \psi_{mn} | \psi_{rs}(T) \rangle$ . Figure 4.5 shows the optimal controls  $v_1(t), v_2(t)$  and  $v_3(t)$  used to obtain the C-not gate. The gate obtained using the  $XXZ$  chain and gate fidelity is as follows

$$\text{C – Not} = \begin{pmatrix} 1 & 0 & 0 & 0 \\ 0 & 1 & 0 & 0 \\ 0 & 0 & 0 & 1 \\ 0 & 0 & 1 & 0 \end{pmatrix}$$

C – Not<sub>xxz</sub> =

$$\begin{pmatrix} 0.9959 + 0.0001i & -0.0015 + 0.0006i & 0.0003 - 0.0003i & -0.0010 - 0.0001i \\ -0.0014 - 0.0010i & 0.9939 - 0.0003i & 0.0015 + 0.0000i & -0.0005 + 0.0005i \\ 0.0013 - 0.0001i & 0.0004 + 0.0003i & 0.0004 - 0.0003i & 0.9945 - 0.0008i \\ -0.0003 - 0.0003i & -0.0013 + 0.0002i & 0.9954 - 0.0004i & 0.0003 + 0.0003i \end{pmatrix}$$

$$\mathcal{F}_{\text{C-Not}} = 0.9949$$

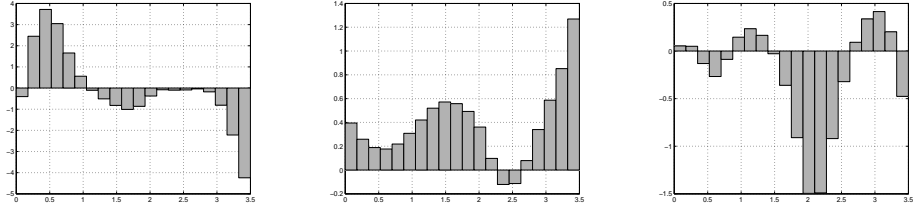


FIGURE 4.5. The C-Not gate controls using two spin- $\frac{3}{2}$  XXZ-chains of length  $L = 50$  at  $\Delta^{-1} = 0.25$  and  $M = 0$  for both the chains. The gate time  $T = 3.5$  is discretized into  $N = 20$  time steps. The figure shows the values for the three control fields  $v_1$ ,  $v_2$  and  $v_3$  that are constant during any one of the time intervals.

## APPENDIX A

## Code

This code constructs single qubit quantum gates on the eigenspace corresponding to the ground state and first excited state pertaining to sector 0 of a spin  $\frac{3}{2}$  XXZ chain with kink boundary conditions. The length of the chain is 8 and  $\Delta^{-1}$  is fixed at 0.3. The control Hamiltonian is a two site operator  $S^3 \otimes S^3$  located at the two middle sites of the chain. The gates are constructed using the optimal control techniques described in chapter 4.

```

%Spin
J=3/2;
%Sector
m=0;
%Length of chain
L=8;
%location of kink for Ising ground state
x=4;
%dimension of Hilbert space at each site
N=2*J+1;
downspins= J*L -m;
%\Delta^{-1} Anisotropy parameter
delta_Inv=0.3;
%time to reach gate
T=10;
%Number of time steps of constant control
N_1=20;
%duration of each time step
delta_t=T/N_1;
%step increase of function in the direction of gradient

```

---

```

step_size =0.2;
%intial controls based on a random guess
u=-0.2*ones(N_1,1);
%u(j)=u(j-1) + step_size*del_u(j)
%The max iterations and threshold of the Gradient ascent algorithm
max_iterations=100;
threshold = 0.0001;
%NOT GATE- X
U_Target_Gate=[0 i; i 0];
%Y GATE
%U_Target_Gate=[0 1; -1 0];
%Z GATE
%U_Target_Gate =[i 0;0 -i];
%HADAMARD GATE - H
%U_Target_Gate=(1/sqrt(2))*[i i; i -i] ;
%PI-8 GATE - T
%U_Target_Gate=[exp(-i*pi/8) 0;0 exp(i*pi/8)]
%PI-8 GATE Adjoint
%U_Target_Gate=[exp(i*pi/8) 0;0 exp(-i*pi/8)]
%PHASE Gate - S
%U_Target_Gate=[exp(-i*pi/4) 0;0 exp(i*pi/4)]
%PHASE GATE Adjoint
%U_Target_Gate=[exp(i*pi/4) 0;0 exp(-i*pi/4)]
% The XXZ Hamiltonian
S3=sparse(1:N,1:N,J-(0:2*J),N,N);
Splus=sparse(N,N);
for j=0:(2*J-1)
    Splus=Splus+sparse(2*J-j,2*J-j+1,sqrt((2*J-j)*(j+1)),N,N);
end
Sminus=transpose(Splus);
%IsingNN = Ising Nearest neighbour interaction

```

---

```

IsingNN=kron(S3,S3);
%HopNN=-kron(Splus,Sminus)-(Sminus,Splus)
HopNN=-kron(Splus,Sminus)-kron(Sminus,Splus);
%IsingH=Ising Hamiltonian
IsingH=sparse(N^L,N^L);
for j=1:(L-1)
    IsingH=IsingH+kron(eye(N^(j-1)),kron(IsingNN,eye(N^(L-1-j))));
end
%HopH=Hopping Hamiltonian
HopH=sparse(N^L,N^L);
for j=1:(L-1)
    HopH=HopH+kron(eye(N^(j-1)),kron(HopNN,eye(N^(L-1-j))));
end
HopH=(1/2)*HopH;
%BdryH=Boundary-field terms
BdryH=kron(S3,eye(N^(L-1)))-kron(eye(N^(L-1)),S3);
%S3tot= total third-component of spin sector
S3tot=sparse(N^L,N^L);
for j=1:L
    S3tot= S3tot+kron(eye(N^(j-1)),kron(S3,eye(N^(L-j))));
end
%The control Hamiltonian
B_1=kron(kron(eye(N^(x-1)),kron(S3,S3)),eye(N^(L-x-1)));
%B_1=kron(kron(kron(eye(N^(x-2)),kron(S3,S3)),S3),eye(N^(L-x-1)));
%We now define the projection to the sector specified by (J*L-downspins)
Proj=speye(N^L);
for j=0:(2*J*L)
    if ne(j,downspins)
        Proj=Proj*(S3tot-(J*L-j)*speye(N^L))/(j-downspins);
    end;
end;

```

---

```

[I,K]=find(Proj);
dim=length(I);
NewProj=sparse(I,1:dim,ones(dim,1),N^L,dim);
NewIsingH=transpose(NewProj)*IsingH*NewProj;
NewHopH=transpose(NewProj)*HopH*NewProj;
NewBdryH=transpose(NewProj)*BdryH*NewProj;
NewBdryH1=transpose(NewProj)*(-J*BdryH/2)*NewProj;
B =transpose(NewProj)*B_1*NewProj;
HIsing=J^2*(L-1)*speye(dim)-NewIsingH + J*NewBdryH ;
A=sqrt(1-(delta_Inv)^2);
HKink=HIsing + delta_Inv *NewHopH + J*(A-1)*NewBdryH;
%two smallest eigenvalues of the XXZ Hamiltonian
[V,D]=eigs(HKink,2,'sa');
%ground state
psi_ground=V(:,1);
%first excited state
psi_excited=V(:,2);
%The XXZ Hamiltonian restricted to the two-dimensional subspace of the
%ground and excited space
H_Kink1 = zeros(2);
H_Kink1(1,1) = psi_ground'*HKink*psi_ground;
H_Kink1(1,2) = psi_ground'*HKink*psi_excited;
H_Kink1(2,1) = psi_excited'*HKink*psi_ground;
H_Kink1(2,2) = psi_excited'*HKink*psi_excited;
%The control Hamiltonian restricted to the two-dimensional subspace of the
%ground and excited space
B_Control = zeros(2);
B_Control(1,1) = psi_ground'*B*psi_ground;
B_Control(1,2) = psi_ground'*B*psi_excited;
B_Control(2,1) = psi_excited'*B*psi_ground;
B_Control(2,2) = psi_excited'*B*psi_excited;

```

---

```

%Main Gradient Ascent Algorithm. Based on a the following paper in Journal
%of Magnetic resonance 'Optimal control of coupled spin dynamics: design of
%MNR pulse sequences by gradient ascent algorithms' JMR 172 (2005) 296-305
phi =0; iterations =0;
clear U
clear X
clear P
while (abs(phi-1) > threshold && iterations < max_iterations)
    for j=1:N_1
        U(:,:,j) = eye(2);
    end
    for j=1:N_1
        X(:,:,j) = eye(2);
    end
    for j=1:N_1
        P(:,:,j) = eye(2);
    end
    for j=1:N_1
        U(:,:,j) = expm(-i*delta_t*(H_Kink1+ u(j)*B_Control));
    end
    for j=1:N_1
        for k=1:j
            X(:,:,j)=U(:,:,k)*X(:,:,j);
        end
    end
    for j=1:N_1
        for k=j+1:N_1
            P(:,:,j)=P(:,:,j)*U(:,:,k)';
        end
        P(:,:,j)=P(:,:,j)*U_Target_Gate;
    end
end

```

---

```

    for j=1:N_1
        del_u(j)= -real(trace(P(:,:,j)')*(i*delta_t*B_Control*X(:,:,j)))/trace(eye(2));
        u(j)=u(j)+step_size*del_u(j);
    end
    phi=real(trace(U_Target_Gate'*X(:,:,N_1)))/trace(eye(2));
    iterations = iterations + 1;
end
clear U_XXZ;
clear U_XXZ_Evolution;
U_XXZ_Evolution = eye(dim);
%Compute the XXZ evolution
for j=1:N_1
    disp('Computing XXZ Evolution ');
    U_XXZ(:,:,j) = eye(dim);
    U_XXZ(:,:,j) = expm(-i*delta_t*(HKink+ u(j)*B));
    U_XXZ_Evolution=U_XXZ_Evolution*U_XXZ(:,:,j);
end
U_XXZ_Gate = zeros(2);
%Restricted to subspace
U_XXZ_Gate(1,1) = psi_ground'*U_XXZ_Evolution*psi_ground;
U_XXZ_Gate(1,2) = psi_ground'*U_XXZ_Evolution*psi_excited;
U_XXZ_Gate(2,1) = psi_excited'*U_XXZ_Evolution*psi_ground;
U_XXZ_Gate(2,2) = psi_excited'*U_XXZ_Evolution*psi_excited;
disp('NOT Gate =');
disp(U_Target_Gate);
disp('Time of Gate T=');
disp(T);
disp('Number of time steps N_1=');
disp(N_1);
disp('XXZ Gate =');
disp(U_XXZ_Gate);

```

```
disp('Iterations of algorithm=');
disp(iterations);
disp('Controls=');
disp(u);
disp('norm(U_XXZ_Gate-U_Target_Gate)=');
disp(norm(U_XXZ_Gate-U_Target_Gate));
disp('(1/2)*trace(|U_Target_Gate - U_XXZ_Gate|)=');
disp(0.5*trace(sqrtm((U_Target_Gate -U_XXZ_Gate)'*(U_Target_Gate-U_XXZ_Gate))));
set(0,'DefaultAxesColorOrder',[0 0 0],...
    'DefaultAxesLineStyleOrder','-|-.|--|:');
hold on
grid on
box on
time = 0;
for j=1:N_1
    area([time;(time+delta_t)], [u(j),u(j)], 'FaceColor', [0.7,0.7,0.7]);
    time =time+delta_t;
end
```

## Bibliography

- [AD01a] F. Albertini and D. D'Alessandro, *The lie algebra structure of spin systems and their controllability properties*, (2001).
- [AD01b] ———, *Notions of controllability for quantum mechanical systems*, Proceedings 40-th Conference on Decision and Control Orlando Florida (2001).
- [AS04] A. Agrachev and Y. Sachkov, *Control theory from the geometric viewpoint*, Springer, 2004.
- [ASW95] F. Alcaraz, S. Salinas, and W. Wreszinski, *Anisotropic ferromagnetic quantum domains*, Nucl Phys B **75** (1995), 930.
- [Be95] A. Barenco and etal, *Elementary gates for quantum computation*, Phys. Rev. A **52** (1995), 3457.
- [BL07] D. Bruss and G. Leuch, *Lectures on quantum information*, Wiley-VCH, 2007.
- [BM05] U. Boscain and P. Mason, *Time minimal trajectories for two-level quantum systems with drift*, Proceedings of the 44th IEEE Conference on Decision and Control, and the European Control Conference (2005).
- [CM03] P. Caputo and F. Martinelli, *Relaxation time of anisotropic simple exclusion processes and quantum Heisenberg models*, Ann Appl Probab **13** (2003), 691.
- [CVZ<sup>+</sup>98] I. Chuang, L. M. K. Vandersypen, X. Zhou, D. Leung, and S. Lloyd, *Experimental realization of a quantum algorithm*, Nature **393** (1998), 143.
- [CZ95] J. Cirac and P. Zoller, *Quantum computations with cold trapped ions*, Phys. Rev. Lett. **74** (1995), 4091.
- [D'A08] D. D'Alessandro, *Introduction to quantum control dynamics*, Chapman and Hall/CRC Applied Mathematics and Nonlinear Science series, 2008.
- [DD01] D. D'Alessandro and M. Dahleh, *Optimal control of two-level quantum systems*, IEEE Transactions on Automatic Control **46** (2001), 866.
- [DKS<sup>+</sup>05] A. Daley, C. Kollath, U. Schollwöck, , and G. Vidal, *Time-dependent density-matrix renormalization-group using adaptive effective hilbert spaces*, Journal of Stat. Mech. **P04005** (2005).
- [ECP08] J. Eisert, M. Cramer, and M. Plenio, *Area laws of entanglement entropy-a review*, (2008), arXiv:0808.3773.
- [FNW92] M. Fannes, N. Nachtergaele, and R. Werner, *Finitely correlated states of quantum spin chains*, Comm. Math. Phys. **144** (1992), 443.

- 
- [Gal07] A. Galiutdinov, *Principles and applications of control in quantum systems*, (2007), arXiv:quant-ph/07051784.
- [GW96] G. Gottstein and R. Werner, *Ground states of the infinite  $q$ -deformed Heisenberg ferromagnet*, (1996), arXiv:cond-mat/9501123.
- [Hal04] B. Hall, *Lie groups, lie algebras, and representations: An elementary introduction*, Springer, 2004.
- [Has07] M. Hastings, *An area law for one dimensional quantum systems*, Journal of Stat. Mech. **P08024** (2007).
- [HHHH07] R. Horodecki, P. Horodecki, M. Horodecki, and K. Horodecki, *Quantum entanglement*, (2007), arXiv:quant-ph/0702225.
- [JS72] V. Jurdjevic and H. Sussman, *Control systems on lie groups*, Journal of Differential Equations **12** (1972), 313.
- [Jur97] V. Jurdjevic, *Geometric control theory*, Cambridge University Press, 1997.
- [Kat82] T. Kato, *Perturbation theory of linear operators*, Springer-Verlag, 1982.
- [KBG01] N. Khaneja, R. Brockett, and S. Glaser, *Time optimal control in spin systems*, Phys Rev A **63** (2001), 032308.
- [Kir04] D. Kirk, *Optimal control theory: An introduction.*, Dover Publications, 2004.
- [KN98] T. Koma and B. Nachtergaele, *The complete set of ground states of the ferromagnetic  $XXZ$  chains*, Adv Theor Math Phys **2** (1998), 533.
- [KNS01] T. Koma, B. Nachtergaele, and S. Starr, *The spectral gap of the ferromagnetic spin- $j$   $XXZ$  chain*, Adv Theor Math Phys **5** (2001), 1047.
- [Kol05] C. Kollath, *The adaptive time-dependent density-matrix renormalization group method: development and applications*, Ph.D. thesis, RWTH Aachen, 2005.
- [KRK<sup>+</sup>05] N. Khaneja, T. Reiss, C. Kehlet, T. Schulte-Herbruggen, and S. Glaser, *Optimal control of coupled spin dynamics: design of nmr pulse sequences by gradient ascent algorithms*, Journal of Magnetic Resonance **172** (2005), 296.
- [LD95] D. Loss and D. DiVincenzo, *Quantum computation with quantum dots*, Phys. Rev. A **57** (1995), 120.
- [Mat95] T. Matsui, *On ground states of the one-dimensional ferromagnetic  $XXZ$  model*, Lett Math Phys **37** (1995), 397.
- [Mes99] A. Messiah, *Quantum mechanics*, Dover Publications, 1999.
- [MK05] H. Mabuchi and N. Khaneja, *Principles and applications of control in quantum systems*, Int J Robust Nonlinear Control **15** (2005), 647.
- [MMK<sup>+</sup>95] C. Monroe, D. Meekhof, B. King, W. Itano, and D. Wineland, *Demonstration of a fundamental quantum logic gate*, Phys. Rev. Lett. **75** (1995), 4714.

- [MMN09] M. Michoel, J. Mulherkar, and B. Nachtergaele, *Implementing quantum gates using the ferromagnetic spin- $j$  XXZ chain with kink boundary conditions*, (2009), arXiv:0902.1276.
- [MNS08] M. Michoel, B. Nachtergaele, and W. Spitzer, *Transport of one-dimensional interfaces in the Heisenberg model*, J. Phys. A **41** (2008), 492001.
- [MNSS08] J. Mulherkar, B. Nachtergaele, R. Sims, and S. Starr, *Isolated eigenvalues of the ferromagnetic spin- $j$  XXZ chain with kink boundary conditions*, Journal of Stat. Mech. **P01016** (2008).
- [MOL<sup>+</sup>99] J. E. Mooij, T. P. Orlando, L. Levitov, T. L., C. H. van der Wal, and S. Lloyd, *Josephson persistent-current qubit*, Science **285** (1999), 1036.
- [NC00] M. Nielsen and I. Chuang, *Quantum computation and quantum information*, Cambridge University Press, 2000.
- [OR95] S. Ostlund and S. Rommer, *Thermodynamic limit of density matrix renormalization*, Phys. Rev. Lett. **75** (1995), 3537.
- [PS90] V. Pasquier and H. Saleur, *Common structures between finite systems and conformal field theories through quantum groups*, Nucl Phys B **330** (1990), 523.
- [Sch05] U. Schollwöck, *The density-matrix renormalization group*, Rev. Mod. Phys. **77** (2005), 259.
- [Sch07] ———, *Progress in density matrix renormalization: What quantum information is teaching us*, Journal of Magnetism and Magnetic Materials **310** (2007), 1294.
- [Sho97] P. Shor, *Polynomial-time algorithms for prime factorization and discrete logarithms on a quantum computer*, SIAM J Comput **26** (1997), 1484.
- [SR72] B. Simon and M. Reed, *Methods of modern mathematical physics, vol. iv: Analysis of operators*, Academic press, 1972.
- [Sta01] S. Starr, *Some properties of the low lying spectrum of the ferromagnetic XXZ chain*, Ph.D. thesis, U.C. Davis, 2001.
- [Vid03] G. Vidal, *Efficient classical simulation of slightly entangled quantum computations*, Phys. Rev. Lett. **91** (2003), 147902.
- [Vid04] ———, *Efficient simulation of one-dimensional quantum many-body systems*, Phys. Rev. Lett. **93** (2004), 040502.
- [WF04] S. White and A. Feiguin, *Real time evolution using the density matrix renormalization group*, Phys. Rev. Lett. **93** (2004), 076401.
- [Whi92] S. White, *Density matrix formulation for quantum renormalization groups*, Phys. Rev. Lett. **69** (1992), 2863.
- [Whi93] ———, *Density-matrix algorithms for quantum renormalization groups*, Phys. Rev. B **48** (1993), 10345.
- [Zab92] J. Zabczyk, *Mathematical control theory: An introduction*, Birkhauser, 1992.
- [ZVSW03] J. Zhang, J. Vala, S. Sastry, and K. Whaley, *Exact two-qubit universal quantum circuit*, Phys. Rev. Lett. **91** (2003), 027903.